Biogeosciences Discuss., doi:10.5194/bg-2016-196, 2016
Manuscript under review for journal Biogeosciences
Published: 14 June 2016

Biogeosciences Discussions
Open Access
EGU

Growth of the coccolithophore *Emiliania huxleyi* in light- and nutrient-limited batch reactors: relevance for the BIOSOPE deep ecological niche of coccolithophores

L. Perrin[1], I. Probert[2], G. Langer[3] and G. Aloisi[4]

[1]Sorbonne Universités, UPMC Univ. Paris 06 -CNRS-IRD-MNHN, LOCEAN-IPSL, 75252 Paris, France.

[2]CNRS-UPMC Univ. Paris 06 FR2424, Roscoff Culture Collection, Station Biologique de Roscoff, 29680 Roscoff, France.

[3]Marine Biological Association, The Laboratory, Citadel Hill, Plymouth PL1 2PB, UK.

[4]LOCEAN, UMR 7159, CNRS-UPMC-IRD-MNHN, 75252 Paris, France.

Correspondence to: L. Perrin (lpelod@locean-ipsl.upmc.fr)

Abstract

Coccolithophores are unicellular, calcifying marine algae that play an important role in the oceanic carbon cycle via their cellular processes of photosynthesis (a CO_2 sink) and calcification (a CO_2 source). Alongside the well-known, shallow-water coccolithophore blooms visible from satellites, deep niches of coccolithophores are a poorly known but potentially important coccolithophore ecosystem. We investigated the conditions that regulate the development of a deep coccolithophore niche (150-200 m depth) along the BIOSOPE transect in the South Pacific oceanic gyre. We carried out batch culture experiments with a coccolithophore strain isolated from the BIOSOPE transect, reproducing the in situ conditions of light- and nutrient- (nitrate and phosphate) limitation. By simulating coccolithophore physiology using an internal stores (Droop) physiological model, we were able to constrain fundamental physiological parameters for this BIOSOPE coccolithophore strain. We show that simple batch experiments, in conjunction with physiological modelling, can provide reliable estimates of fundamental physiological parameters that are usually obtained in more time consuming and costly chemostat experiments. The combination of culture experiments, physiological modelling and in situ data from the BIOSOPE cruise show that coccolithophore growth in the deep BIOSOPE niche is co-limited by availability of light and nitrate. This study contributes to the understanding of *Emiliania huxleyi* physiology, metabolism and behavior in a disadvantageous ecosystem of the ocean.

Keywords

Coccolithophores, batch cultures, Deep niche, South Pacific Gyre, Droop model.

Biogeosciences Discuss., doi:10.5194/bg-2016-196, 2016
Manuscript under review for journal Biogeosciences
Published: 14 June 2016

1. Introduction

Coccolithophores are unicellular photosynthetic and calcifying organisms that play a key role in the global carbon cycle (Paasche, 2001; Winter and Siesser, 1994). Through photosynthesis they participate to the upper ocean carbon pump (CO_2 sink), while via calcification they participate to the carbonate counter-pump (CO_2 source) (Paasche, 2001; Westbroek et al., 1993). The relative importance of calcification and photosynthesis dictates the effect coccolithophores have on ocean-atmosphere CO_2 fluxes (Shutler et al., 2013). Environmental conditions such as temperature, irradiance, nutrient concentrations and pCO_2 exert a primary control on the calcification/photosynthesis ratio (PIC:POC); and also affect coccolithophore biogeography via their influence on cellular growth rates. Together, these effects modulate the impact of coccolithophores on ocean-atmosphere CO_2 fluxes.

Despite the fact that certain coccolithophores have been fairly extensively studied in the laboratory (Daniels et al., 2014; Iglesias-Rodriguez et al., 2008; Krug et al., 2011; Langer et al., 2012; Rouco et al., 2013), the factors controlling their biogeography in the global ocean are poorly understood (Boyd et al., 2010). In controlled laboratory conditions, coccolithophore growth is monitored as given environmental parameters are varied (Buitenhuis, 2008; Feng et al., 2008; Fritz, 1999; Langer et al., 2006; Leonardos and Geider, 2005; Paasche, 1999; Trimborn et al., 2007). In the ocean, geographical surveys of coccolithophore abundance and concomitant measurements of environmental variables contribute to defining coccolithophore biogeography in relation to the environment (Claustre et al., 2008; Henderiks et al., 2012). However, extrapolation of results from laboratory experiments to interpret field distributions is not straightforward, primarily because multiple environmental variables co-vary spatially in the ocean (Henderiks et al., 2012; Poulton et al., 2014).

In this respect, one of the least well understood, but possibly globally relevant niches where coccolithophores can be relatively abundant is that occurring at the deep nutricline of oceanic gyres. The deep niche of coccolithophores discovered during the BIOSOPE cruise in the South Pacific Gyre (Beaufort et al., 2007; Claustre et al., 2008) is probably the best studied example. This deep coccolithophore niche occurred at around the 200 m nutricline, at very low irradiance levels (< 20 $\mu mol.m^{-2}.s^{-1}$) with dissolved nitrate (NO_3) and phosphate (PO_4) concentrations of about 1 µM and 0.2 µM, respectively, and was dominated by coccolithophore species belonging the family Noëlaerhabdaceae: *Emiliania huxleyi* , and several species of G*ephyrocapsa* and *Reticulofenestra* (Beaufort et al., 2007). Deep-dwelling (> 80 m depth) coccolithophores have also been observed in other geographic regions. Okada and McIntyre (1979) observed coccolithophores in the North Atlantic Ocean down to a depth of 100 m where *Florisphaera profunda* dominates coccolithophore assemblages in summer and *E. huxleyi* for the rest of the year. Coccolithophore assemblages dominated by *F.profunda* in the lower photic zone (LPZ > 100 m) of the subtropical gyres were observed by Cortés et al. (2001) in the Central North Pacific Gyre (station ALOHA)

Biogeosciences Discuss., doi:10.5194/bg-2016-196, 2016
Manuscript under review for journal Biogeosciences
Published: 14 June 2016

and by Haidar and Thierstein (2001) in the Sargasso Sea (North Atlantic Ocean). Jordan and Winter (2000) reported deep populations of coccolithophores dominated by *F. profunda* in the LPZ in the north-east Caribbean but also reported a high abundance and co-dominance of *E. huxleyi* and *G.oceanica* through the water column down to the top of the LPZ. These deep-dwelling coccolithophores are not recorded by satellite-based remote sensing methods (Henderiks et al., 2012; Winter et al., 2014) that detect back-scattered light from coccoliths from a layer only a few tens of meters thick at the surface of the ocean (Holligan et al., 1993; Loisel et al., 2006).

Understanding the development of deep coccolithophore populations in low nutrient, low irradiance environments would contribute to building a global picture of coccolithophore ecology and biogeography. Laboratory cultures with coccolithophores that combine both nutrient and light limitation, however, are scarce. One reason is that investigating phytoplankton growth under nutrient limitation in laboratory experiments is complicated (Langer et al., 2013). In batch cultures the instantaneous growth rate decreases as nutrients become limiting, making it hard to extract the dependence of growth rate on nutrient concentrations (Langer et al., 2013). Chemostat cultures, where growth rates and nutrient concentrations are kept constant under nutrient-limited conditions, offer an alternative (Engel et al., 2014; Leonardos and Geider, 2005; Müller et al., 2012). Physiological parameters obtained in chemostat experiments have been used in biogeochemical models to investigate environmental controls on phytoplankton biogeography (Follows and Dutkiewicz, 2011; Gregg and Casey, 2007). Unfortunately, despite their relevance to nutrient limited growth, chemostat cultures are more expensive, time-consuming and complicated to set up than batch cultures (LaRoche et al., 2010).

In this paper, we investigate the growth of the coccolithophore *E. huxleyi* under light and nutrient co-limitation with the aim of understanding the environmental controls on the development of deep populations of this species discovered during the BIOSOPE cruise (Beaufort et al., 2007). We carried out batch culture experiments with an *E. huxleyi* strain isolated during the BIOSOPE cruise and reproduced low light and low nutrient conditions approaching the in situ values of the deep ecological niche. We monitored the nitrogen and phosphorus content of particulate organic matter, as well as cell, coccosphere and coccolith sizes, because these parameters are known to vary systematically with nutrient limitation (Fritz, 1999; Kaffes, 2010; Rouco et al., 2013). To overcome the conceptual limitations inherent in nutrient-limited batch experiments (Langer et al., 2013), we modelled the transient growth conditions in the batch reactor assuming that assimilation of nutrients and growth are either coupled (Monod, 1949) or decoupled (Droop, 1968) processes in the coccolithophore *E. huxleyi*. An independent check of our modelling approach was obtained by also modelling the *E. huxleyi* batch culture data of Langer et al. (2013). Our joint culture and modelling approach provides information on the conditions that control the growth of *E. huxleyi* in the deep ecological niche of the South Pacific Gyre, and demonstrate that batch experiments, if conducted

Biogeosciences Discuss., doi:10.5194/bg-2016-196, 2016
Manuscript under review for journal Biogeosciences
Published: 14 June 2016

thoroughly, may provide valuable estimates of fundamental physiological parameters that are otherwise obtained via more time-consuming and costly chemostat experiments (LaRoche et al., 2010).

2. Materials and methods

2.1 Experimental

2.1.1 Growth medium and culture conditions

Natural seawater collected near the Roscoff Biological Station (Brittany, France) was sterile filtered and enhanced to K/2(-Si,-Tris) medium according to Keller et al. (1987). *Emiliania huxleyi* strain RCC911, isolated in summer 2004 from a sample collected at 10 m depth near the Marquesas Islands during the BIOSOPE cruise, was grown in batch cultures. Cells were acclimated to experimental conditions for at least three growth cycles. Experiments were conducted in triplicate in 2.7 litre polycarbonate bottles (Nalgene) with no head space, under a 12:12 light:dark irradiance cycle and at a temperature of 20°C. The concentration of dissolved nitrate (NO_3) and phosphate (PO_4) and the irradiance levels were chosen to reproduce the conditions prevalent in surface waters and at the nitricline of the oligotrophic gyre in the South Pacific Ocean (Morel et al., 2007). The high light condition was 140 $\mu mol.m^{-2}.s^{-1}$ and the low light condition was 30 $\mu mol.m^{-2}.s^{-1}$. The low irradiance condition was at the upper end of the irradiance range (10-30 $\mu mol.m^{-2}.s^{-1}$) in the deep BIOSOPE coccolithophore niche and we chose not to run experiments at irradiance levels lower than this to avoid very long experimental runs. Nutrient concentrations at the beginning of batch experiments were 100 µM and 2.5-5.1 µM for nitrate and 6.25 and 0.45-0.55 µM for phosphate in nutrient-replete and nutrient-limited conditions, respectively. For each irradiance level, three experiments were carried out (in triplicate): control (nutrient-replete), phosphate limited (P-limited) and nitrate limited (N-limited) conditions.

2.1.2 Cell enumeration and growth rate

The growth of batch cultures was followed by conducting cell counts every day or every other day using a BDFacs Canto II Flowcytometer. Experiments were stopped before the cell density reached ca. $1.5*10^5$ $cells.mL^{-1}$ in order to minimize shifts in the dissolved inorganic carbon (DIC) system. Cultures remained in the exponential growth phase throughout the duration of the control (nutrient-replete) experiments. In these control cultures, the growth rate (µ) was obtained by conducting a linear regression of the cell density data on the logarithmic scale. Nutrient-limited experiments were allowed to run until growth stopped. The growth rate in nutrient limited conditions decreases in time as nutrients are depleted and it is therefore not possible to calculate growth rate by means of regression analysis (Langer et al., 2013). The dependence of growth rate on nutrient concentration in nutrient-limited conditions was investigated with the numerical model introduced in Sect. 2.2 below.

Biogeosciences Discuss., doi:10.5194/bg-2016-196, 2016
Manuscript under review for journal Biogeosciences
Published: 14 June 2016

2.1.3 Cell, coccosphere diameter and coccolith length

Samples were taken at the end of the experiments to acquire images of cells using an optical microscope (x100, oil immersion, Olympus BX51 microscope). The internal cell diameter of 100 cells was measured for each experimental culture using the ImageJ software (http://rsbweb.nih.gov/ij/). Images of coccospheres and coccoliths were obtained with scanning electron microscopy (SEM). For SEM observations, samples were filtered onto 1.2 µm polycarbonate filters (Millipore), rinsed with a basic solution (180 µL of ammomia solution 25 % in a liter of MilliQ water) and dried at 55°C for 1 h. After mounting on an aluminum stub, they were coated with gold-palladium and images were taken with a Phenom G2 pro desktop Scanning Electron Microscope. For each experimental culture 100 coccospheres were measured using ImageJ. Three hundred coccoliths per sample were measured using a script (Young et al., 2014) that is compatible with ImageJ in order to measure the distal shield length (DSL) and coccolith width.

2.1.4 Dissolved inorganic carbon (DIC) and nutrient analyses

Subsamples for pH_T (pH on the total scale), DIC and nutrient analyses were taken from culture media at the beginning and at the end of each experiment. The pH was measured with a pHmeter-potentiometer pHenomenal pH1000L with a Ross ultra combination pH electrode on the total scale and was calibrated with a TRIS buffer. Samples for the determination of DIC were filtered through pre-combusted glass-fibre filters (Whatman GF/F) into acid-washed glass bottles and poisoned with mercuric chloride. Bottles were stored at 4°C prior to analysis. A LICOR7000 CO_2/H_2O gas analyzer was used for the DIC analysis (precision ± 2 µmol.kg^{-1}). A culture aliquot (100 mL) was filtered onto pre-combusted glass-fibre filters (Whatman GF/F) and then stored at -20°C in a polyethylene flask until nutrient analysis. Nitrate and phosphate concentrations were measured using a CHN Auto analyzer Seal Analytical AAIII (detection limits were 0.003 µM for PO_4 and 0.01 µM for NO_3).

2.1.5 POC, PON, PIC, POP

For particulate organic carbon (POC), particulate organic nitrogen (PON), particulate inorganic carbon (PIC) and particulate organic phosphorus (POP) analyses, samples (200 or 250mL) were filtered onto pre-combusted (4 h at 450°C) glass-fibre filters (Whatman GF/F) and preserved at -20°C. POC and PON were measured on the same filter that was dried overnight at 50°C after being placed in a fuming hydrochloric acid dessicator for 2 h to remove coccolith calcite. POC and PON were analyzed using a NC Analyzer Flash EA 1112. PIC was obtained using a 7500cx Agilent ICP-MS by analyzing the calcium concentration on the glass-fibre filter (Whatman GF/F) extracted by a solution of hydrochloric acid. POP was determined as the difference between the total particulate phosphorus and the particulate inorganic phosphorus, analyzed according to the method of Labry et al. (2013).

Biogeosciences Discuss., doi:10.5194/bg-2016-196, 2016
Manuscript under review for journal Biogeosciences
Published: 14 June 2016

2.2 Modelling

2.2.1 Monod and Droop model

Growth of *E. huxleyi* in the batch reactors was simulated using Monod and Droop models of cellular growth. In the Monod model (Monod, 1949), the growth rate depends on the external nutrient concentration and is calculated as:

$$\mu = \mu_{\max} \cdot \frac{[N]}{[N] + K_N} \quad (1)$$

where μ_{max} (in day^{-1}) is the maximum growth rate in nutrient-replete conditions, K_N (in µmol.L^{-1}) is the (Monod) half-saturation constant for growth and *[N]* (in µmol.L^{-1}) is the concentration of nutrient N in the batch reactor. Both μ_{max} and K_N were obtained by fitting the model to the data, while *[N]* was the nutrient concentration measured in the culture experiments.

Two differential equations keep track of the total cell abundance in the batch reactor (*Cells*) and the limiting nutrient concentration in the reactor:

$$\frac{dCells}{dt} = \mu \cdot Cells \quad (2)$$

$$\frac{d[N]}{dt} = \frac{-N_{FIX} \cdot Cells}{V_R}$$

where V_R (in litres) is the volume of the batch reactor, *Cells* (in cell.mL^{-1}) is the cell density measured during the experiments, and N_{FIX} the cell-specific N fixation rate (in µmol$_N$.cell^{-1}.day^{-1}) given by:

$$N_{FIX} = \mu \cdot Q_N \quad (3)$$

where Q_N, the (constant) cellular quota of nutrient N (in µmol$_N$.cell^{-1}), was calculated from the cellular carbon quota, Q_C (in µmol$_C$.cell^{-1}) (measured in experiments) and the C/N ratio obtained by the Redfield ratio (Redfield, 1963).

In the Droop model (Droop, 1968) nutrient uptake and cellular growth are decoupled and cellular growth depends on the internal store of the limiting nutrient. The time-dependent rate of nutrient uptake, N_{up} (in µmol$_N$.cell^{-1}.day^{-1}), is simulated using Michaelis-Menten uptake kinetics:

$$N_{up} = S_{cell} \cdot V_{\max} \cdot \frac{[N]}{[N] + K_N} \quad (4)$$

where S_{Cell} (in µm^3) is the surface area of the cell, V_{max} (in µmol$_N$.µm^{-2}.d^{-1}) is the maximum surface-normalized nutrient uptake rate (obtained by fitting the model to the data) and K_N (in µmol.L^{-1}) is the

Biogeosciences Discuss., doi:10.5194/bg-2016-196, 2016
Manuscript under review for journal Biogeosciences
Published: 14 June 2016

(Michaelis-Menten) half-saturation constant for uptake of nutrient N. The volume and surface of cells (S_{cell}) was either obtained by measurements of cells (both in the control culture and at the end of the nutrient-limited cultures) or was estimated from Q_C, the cellular organic carbon quota (in $pmol_C.cell^{-1}$), and the density of carbon in coccolithophore biomass (approximately equal to 0.015 $pmol_C\ \mu m^{-3}$) (Aloisi, 2015). The phytoplankton growth rate μ (in d^{-1}) was calculated based on the normalized ^{n}Quota equation reported in (Flynn, 2008):

$$\mu = \mu_{\max} \cdot \frac{(1+KQ)\cdot(Q-Q_N^{\min})}{(Q-Q_N^{\min})+KQ\cdot(Q_N^{\max}-Q_N^{\min})} \quad (5)$$

where μ_{max} (in $days^{-1}$) is the maximum growth rate attained at the maximum nutrient cell quota Q_N^{min} (in $\mu mol\ cell^{-1}$), Q_N^{min} (in $\mu mol\ cell^{-1}$) is the minimum (subsistence) cellular quota of nutrient N below which growth stops and *KQ* is a dimensionless parameter that can be readily compared between nutrient types and typically has different values for NO_3 and PO_4 (Flynn, 2008). While Q_N^{max} and Q_N^{min} were obtained from the analyses of the particulate organic quota of the nutrient (NO_3 or PO_4) at the beginning and at the end of the experiments, *KQ* was obtained from fitting the model to the data. Thus, the growth rate depends on the internal cellular quota of nutrient N, rather than on the external nutrient concentration like in the Monod model of phytoplankton growth.

Three differential equations keep track of the total cell abundance in the batch reactor (*Cells*), the nutrient concentration in the reactor (*[N]*, in $\mu mol.L^{-1}$) and the internal cellular quota of nutrient (Q_N, in $\mu mol.\ cell^{-1}$):

$$\frac{dCells}{dt} = \mu \cdot Cells \quad (6)$$

$$\frac{d[N]}{dt} = \frac{-N_{up}\cdot Cells}{V_R} \quad (7)$$

$$\frac{dQ_N}{dt} = N_{up} - \mu \cdot Q_N \quad (8)$$

These three differential equations are integrated forward in time starting from initial conditions chosen based on experimental values of the number of cells, nutrient concentration at the beginning of the experiment and the cellular nutrient quota determined during growth in nutrient-replete conditions.

The dependence of the maximum growth rate on irradiance was determined independently by fitting the growth rate determined in the exponential growth phase in our experiments and in the experiment of Langer et al. (2013) to the following equation from MacIntyre et al. (2002):

Biogeosciences Discuss., doi:10.5194/bg-2016-196, 2016
Manuscript under review for journal Biogeosciences
Published: 14 June 2016

$$\mu = \mu_{\max}\left(1 - e\left(\frac{-Irr}{KIrr}\right)\right) \quad (9)$$

where KIrr is the light-saturation parameter of growth in µmol.m^{-2}.s^{-1} (MacIntyre et al., 2002; Fig. 1).

2.2.2 Modelling strategy

The Droop model presented here does not take into account the variation of size of coccolithophore cells between the different experiments.

This model has eight parameters. Four are considered to be known and constant for a given experiment: batch volume V_R, cell volume (and surface area S_{Cell}), and minimum and maximum cellular quota of nutrient, respectively Q_{min} and Q_{max}. The unknown parameters (the physiological parameters of interest) are: the (Michaelis-Menten) half-saturation constant for nutrient uptake $K_{N/P}$, the maximum surface-normalized nutrient uptake rate V_{max}, the maximum growth rate μ_{max} and the dimensionless parameter KQ (N or P). The Monod model has fewer known parameters: batch volume V_R and cellular quota of nutrient $Q_{N/P}$. Unknown parameters are: maximum growth rate μ_{max} and the (Monod) half-saturation constant for growth $K_{N/P}$.

The time-dependent cell density, limiting nutrient concentration and cellular particulate organic nitrogen and phosphorus calculated by the models were fitted to the same quantities measured in the experiments. For our experiments there were only two nutrient data points, one at the beginning and one at the end of the experiments. We artificially inserted a third nutrient-quota data point at the end of the exponential growth phase, setting it equal to the nutrient quota at the beginning of the experiment. In this way the model is forced to keep the nutrient quota unchanged during the exponential growth phase. This is a reasonable assumption, as cellular nutrient quotas should start to be affected only when nutrient conditions become limiting.

The quality of the model fit to the experimental data was evaluated with a cost function. For a given model run, the total cost function was calculated as follows:

$$TotCost = \sum_{i=1}^{n} (\Delta x_i)^2 \quad (10)$$

where n is the number of data points available and Δx_i is the difference between the data and the model for the ith data point:

$$\Delta x_i = Data(x_i) - Model(x_i) \quad (11)$$

where x_i is the data or model value for the considered variable (cell density, limiting nutrient concentration or cellular limiting nutrient quota). The lower the cost function is, the better the quality of the model fit to

Biogeosciences Discuss., doi:10.5194/bg-2016-196, 2016
Manuscript under review for journal Biogeosciences
Published: 14 June 2016

the data. For a given experiment, the best-fit of the model to the data was obtained by running the model repeatedly imposing a high number of combinations of input parameters (typically 500000 model runs for every experiment) and selecting the parameter setting that yielded the lowest cost.

3. Results

3.1 Laboratory experiments with E. huxleyi strain RCC911

3.1.1 Cell density and growth rate

Growth curves for all experiments with *E. huxleyi* strain RCC911 are shown in Fig. 2. Experiments run in high light conditions attained target cell densities (in nutrient-replete, control experiments) or nutrient limitation (in nutrient-limited experiments) in a shorter time compared to experiments run in low light conditions. Growth in nutrient-replete cultures in both light conditions followed an exponential growth curve (growth rates in the control nutrient-replete experiments were 0.91 ± 0.03 d^{-1} and 0.28 ± 0.01 d^{-1} for the high light and low light experiments, respectively; Table 1) whereas in nutrient-limited experiments growth evolved from an exponential to a stationary phase at the end of the experiment, except the P-limited culture at low light where the stationary phase was not attained (growth rate of 0.13 ± 0.01 d^{-1}).

3.1.2 Dissolved nutrients, pH_T and DIC

In the high light experiment, NO_3 concentration decreased to 0.18 ± 0.03 µM in N-limited cultures and PO_4 concentration decreased to 0.011 ± 0.004 µM in P-limited cultures at the end of the experiments, and in low light conditions the final NO_3 and PO_4 concentrations were 0.13 ± 0.02 µM and 0.008 ± 0.006 µM, respectively (Table 1). Thus, nutrients where nearly completely exhausted at the end of our nutrient-limited experiments. Seawater carbonate chemistry was quasi-constant over the course of the experiments in all treatments, with as reported by Langer et al. (2013), the P-limited cultures showing the biggest change in DIC (12-13%; Table 1).

3.1.3 Carbon, nitrogen and phosphorus cell quotas and ratios

Compared to the control experiments, cellular POC, PIC and PON quotas increased in the P-limited cultures at both light levels,, while cellular POP quota decreased (Table 2; Fig. 3). In the N-limited cultures, cellular PIC and POC quotas increased, with the exception of POC at low light that remained nearly unchanged, while cellular PON and POP quotas decreased at both light levels. N-limiting conditions resulted in a decrease of the PON:POC ratio in both light regimes (Fig. 4A, Table 2). Changes in the POP:POC ratio (Fig. 4*Figure 4*B, Table 2) were harder to discern due to a large error bar in high light and nutrient-replete conditions. Notwithstanding, POP:POC was lower in P-limited experiments compared to nutrient-replete experiments. The PIC:POC ratio increased with both N- and P-limitation (Fig. 4C) at both light regimes. For the high light experiment, the PIC:POC ratio was highest in the P-limited culture (0.52 ± 0.14), while in the

Biogeosciences Discuss., doi:10.5194/bg-2016-196, 2016
Manuscript under review for journal Biogeosciences
Published: 14 June 2016

298 low light conditions, the highest ratio was recorded in the N-limited culture (0.33 ± 0.02) (Fig. 4C).
299 Light limitation led almost invariably to a decrease in POC and PIC, with the exception of POC in nutrient-
300 replete conditions, for which the decrease in irradiance did not induce a decrease (Table 2, Fig. 3). In P-
301 limited cultures POP and PON decreased with light limitation, whereas in N-limited cultures POP and PON
302 increased with light limitation (Fig. 3). With the exception of the POP:POC ratio in P-limiting conditions that
303 was not affected by the change in light regime, both PON:POC and POP:POC ratios increased with light
304 limitation. In all three nutrient conditions, the PIC:POC ratio decreased with light limitation.
305

306 **3.1.4 Cell, coccosphere and coccolith size**
307 Cell size varied with both nutrient and light limitation (Table 3). In high light conditions the cell volume was
308 higher for the P-limited culture, with a volume of 77.2 ± 19.9 μm^3, than for the control culture and the N-
309 limited culture that had similar cell volumes (ca. 47-50 μm^3). Cell volume was consistently lower in low light
310 conditions, and P-limited cultures again had higher cell volume than in the control and N-limited cultures.
311 POC content and cell volume is illustrated in Fig. 5A (R^2=0.75, p<0.006, n=8).
312 P-limitation resulted in higher coccosphere volume and higher DSL than the other nutrient conditions in
313 both light regimes (Table 3). For example, the coccosphere volume in high light was 260 ± 88 μm^3 for the P-
314 limited experiment, whereas it was 109 ± 23 μm^3 for the control experiment and 139 ± 41 μm^3 for the N-
315 limited experiment. There was no measurement of coccosphere volume and DSL in the low light control
316 culture because of a lack of cells on the filters. However, the coccosphere volume for P-limited in low light
317 conditions followed the same trend as the cell size, a decrease with lower light. Figure 5B shows the
318 correlation between cell and coccosphere volume (R^2=0.90, p<0.002, n=7). The correlations between DSL
319 and coccosphere size (R^2=0.73, p<0.05, n=7) and between the DSL and the cell size (R^2=0.85, p<0.003, n=7)
320 are illustrated in Fig. 6.
321 The thickness of the coccolith layer, calculated by subtracting the cell diameter from the coccosphere
322 diameter and dividing by two, was higher for P-limited cultures in both light conditions: 1.294 ± 0.099 µm
323 for high light and 1.02 ± 0.043 µm for low light compared with the other cultures which were between 0.66
324 and 1 µm. This observation is consistent with the high PIC quota and relatively large size of coccospheres
325 and coccoliths of *E. huxleyi* under P-limitation.
326

327 ***3.2 Modelling results***
328
329 We applied the modelling approach to both the data from our batch culture experiments with strain
330 RCC911 and to the batch culture data of Langer et al. (2013) who tested N- and P-limited growth of *E.*
331 *huxleyi* strain PML B92/11 cultured in high light conditions (400 $\mu mol.m^{-2}.s^{-1}$), optimal temperature (15°C)
332 and quasi-constant carbon system conditions. Measurements of cell density, nutrient concentrations and
333 cellular particulate matter from both sets of experiments were used for the present modelling study.

Biogeosciences Discuss., doi:10.5194/bg-2016-196, 2016
Manuscript under review for journal Biogeosciences
Published: 14 June 2016

334 The measured minimum PON value (5.71 fmol cell^{-1}) for the N-limited experiment of Langer et al. (2013) is
335 very low compared with the PON quota in other N-limited *E. huxleyi* experiments reported in the literature
336 (38.9-39.3 fmol.cell^{-1} in Sciandra et al. (2003) and 51.4 fmol.cell^{-1} in Rouco et al. (2013)). When the Q_N^{min}
337 value of Langer et al. (2013) was used in the model, the model fit to the experimental data degraded
338 considerably (data not shown). Consequently, we decided to recalculate Q_N^{min} using the initial
339 concentration of dissolved N and the final cell density in the reactor (column "Calculation"in Table 4). This
340 calculated value of Q_N^{min}, that in all cases except for the N-limited experiments of Langer et al. (2013) was
341 very similar to the measured minimum PON quota, was comparable to values reported in the literature for
342 *E. huxleyi* and resulted in a very good fit of the model to the experimental data. To be coherent, we applied
343 this approach to all values of Q_N^{min} and Q_P^{min} used in the modelling exercise.
344
345 The Droop model was able to accurately reproduce both experimental data sets (Fig. 7 to 11), whereas the
346 Monod model was not able to reproduce the rise in cell number after the limiting nutrient had been
347 exhausted (Fig. 7). The modelling approach allows evaluation of the evolution of experimental variables
348 that are complicated to determine analytically (Fig. 7 to 11), i.e.: 1) the nutrient-uptake rate, that follows
349 the same trend as the nutrient concentration in the reactor; (2) the limited-nutrient/C ratio, that starts at a
350 maximum value, stays constant during the duration of the exponential phase and then declines due to the
351 exhaustion of external nutrient, reaching a minimum as the culture attains the stationary phase, and (3) the
352 instantaneous growth rate, that follows the trend of the limiting nutrient ratio, reaching zero when the
353 culture attains the stationary phase.
354
355 The values for the best-fit for physiological parameters obtained by applying the Droop model to our
356 experiments with *E. huxleyi* strain RCC911 and to the experiments of Langer et al. (2013) are presented in
357 Table 4. Overall, the best-fit values for the two strains were similar, suggesting that the modelling approach
358 is sound. Values for the Monod nutrient assimilation constant K_N determined in our experiments and in
359 those of Langer et al. (2013) were comparable. However, for K_P, the value was consistent between our high
360 and low light experiments, but considerably lower for the Langer et al. (2013) experiment. The same holds
361 true for the maximum surface nutrient-uptake rate V_{max} (except for our P-limited low light experiment). The
362 dimensionless parameters KQ_N and KQ_P were comparable between the two studies (for high light
363 conditions) and in both cases KQ_P was higher than KQ_N. Maximum growth rates in high light conditions
364 were similar for both N-limited and P-limited experiments. As expected, the maximum growth rate for our
365 low light cultures was considerably lower.
366 To test the reliability of the model to obtain estimates of the physiological parameters, we forced the
367 model to run with a range of values for a given parameter, while letting the other three parameters vary
368 over a wide range, obtaining plots of the value of the cost function (Eq. 9) as a function of the value of the
369 imposed parameter. The process was repeated separately for the four unknown parameters (Fig. 12) shows

Biogeosciences Discuss., doi:10.5194/bg-2016-196, 2016
Manuscript under review for journal Biogeosciences
Published: 14 June 2016

the results for the N-limited culture of Langer et al. (2013). For all of the parameters except for $K_{N/P}$, this exercise yielded a U-shaped curve with a minimum of the cost function corresponding to the best-fit parameter values presented in Table 4. This shows that the model is well suited to find a best-fit value of these parameters. Three minima of the cost function were found for $K_{N/P}$ (Fig. 12) of which only the lowest was consistent with values reported in the literature (Riegman et al., 2000). This value was chosen to obtain the best-fit of the model to the experimental data.

4. Discussion

4.1 Batch culture experiments

The batch culture experiments presented here provide new insights into the physiology of the ecologically dominant coccolithophore *E. huxleyi* under conditions of light and nutrient limitation that are relevant for the study of deep coccolithophore niches. Leonardos and Geider (2005) carried out cultures in low light and low phosphate conditions, but they did not measure PIC and thus did not report PIC:POC ratios. The culture study reported here is thus the first experiment where changes in the PIC:POC ratio due to light-limitation are explored for nutrient-limited cultures.

In our experiments, cultures were harvested at relatively low cell densities (maximum of ca. $1.6*10^5$ cells.mL^{-1} in the P-limited low light experiment, and < $1.3*10^5$ cells.mL^{-1} in all other treatments) in order to ensure that changes in the carbonate system were within a minimal range (generally < 10%; Table 1) that is not expected to have a significant influence on measured physiological parameters (Langer et al., 2007; LaRoche et al., 2010). Hence, it can be stated that the observed phenomena stem from N-/P-limitation and/or light limitation (depending on the treatment) rather than from carbon limitation.

Comparison of the growth curves illustrated in Fig. 2 demonstrates that growth limitation was attained in both our low nutrient and low light treatments relative to control (high nutrient / high light) conditions. Consistent with previous experimental results (Langer et al., 2013; Leonardos and Geider, 2005; Müller et al., 2012; Oviedo et al., 2014; Rouco et al., 2013) the relatively low cellular PON or POP quotas (and PON:POC and POP:POC ratios) at the end of the low nutrient experiments indicate that nutrient limitation of growth occurred in our low nutrient experiments. The stationary phase was not attained in the phosphate-limited low light culture, but the very low POP quota (and POP: POC ratio) and increased cell size indicate that P-limitation was starting to significantly affect cellular physiology, showed as well by the decrease in growth rate between the nutrient-replete conditions in low light and this experiment.

In nutrient-replete conditions, low light had no effect on POC quota (Fig. 3) and cell size (Fig. 5) within the limit of uncertainty of measurements. In same nutrient condition, low light did however cause a decrease in PIC quota (and therefore a decrease in the PIC:POC ratio). Although the same observation will be done for nutrient-limited conditions in low light in the following paragraphs, the quota for nutrient-replete

conditions in low light is unexpectedly small and the lack of measurements for coccospheres and coccoliths size show a potential problem in the calcification process for this experiment.

In high light, N-limited cells were roughly the same size as nutrient-replete cells but had higher POC quota. However, large error margins do not allow explaining these observations as the density in $pg.\mu m^{-3}$ calculated shows no significant difference between experiments. In low light, N-limited cells were similar in size and POC quota to nutrient-replete cells. According to Müller et al. (2008), N-limited cells decrease in volume due to substrate limitation and lower assimilation of nitrogen in the G1 phase of the cell division cycle, but in our experiments N-limitation did not cause a decrease in cell volume. N-limitation led to an increase in PIC quota relative to nutrient-replete cells in both high and low light conditions (Fig. 3) (Table 3). Fritz (1999) reported as well an increase of PIC content in N-limited conditions as Müller et al. (2008). However, Raven and Crawfurd (2012) affirm that N-limitation lead to a reduced biomass rather than calcite which lead as well to a decreasing in cell size. Coccoliths in N-limited cultures tended to be smaller (in line with the observations of Paasche, 1998) and coccosphere volumes tended to be higher than in nutrient-replete cultures (large uncertainties of measurements), so N-limited cells presumably produced more coccoliths. N-limitation led to an increase in the PIC:POC ratio in both high and low light conditions, a result that is consistent with most previous N-limitation studies with *E. huxleyi* (see review by Raven and Crawfurd, 2012).

P-limitation had the greatest effect on cell size, cells being significantly larger under P-limitation than control conditions in both high and low light conditions. The increase in cell volume was accompanied by increases in both POC and PIC quotas (Fig. 3). According to Müller et al. (2008), P-limitation inhibits DNA replication while biomass continues to build up, leading to an increase in cell volume. This could explain why the volume of P-limited cells in high light was very high in our experiments, but our results indicate that when growth was already limited by light availability, P-limited cells were not as large, had correspondingly lower POC and POP quotas, and were able to continue dividing beyond the cell density at which growth was limited in high light conditions, thus representing an interesting case of the combined effects of co-limitation. P-limitation resulted in considerably higher coccosphere volume than the other nutrient conditions, in line with the observations of Müller et al. (2008) and Oviedo et al. (2014). In high light the PIC quota in P-limited cells was more than tripled relative to nutrient-replete conditions (general effect of a phosphate limitation reported by Raven and Crawfurd (2012) (Table 2), likely due to the occurrence of larger (as shown by high DSL values) and potentially more numerous coccoliths (Gibbs et al., 2013).

In the P-limited experiment, PIC:POC ratios increased relative to nutrient-replete cultures, like in the experiments of van Bleijswijk et al. (1994) and Berry et al. (2002), although Oviedo et al. (2014) reported

441 that the response of the PIC:POC ratio to P-limitation is strain-specific in *E. huxleyi*. The increase in PIC:POC
442 in *E. huxleyi* is often greater for decreasing phosphate than for decreasing nitrate (Zondervan, 2007), as was
443 the case in our high light experiment, but in low light the PIC:POC ratio was higher under N-limitation, again
444 highlighting that co-limitation can have unexpected physiological consequences.
445
446 The PIC:POC ratio decreased with light limitation in nutrient replete and nutrient limited conditions in our
447 experiment (Fig. 4). In a review of environmental effects on coccolithophore calcification, Zondervan (2007)
448 stated that due to the lower saturation irradiance for calcification than photosynthesis in *E. huxleyi*, the
449 ratio of calcification to photosynthetic C fixation increases with decreasing light intensities. However, due
450 to a more rapid decline of calcification relative to photosynthesis this ratio decreases again under strongly
451 light-limiting conditions (below approximately 30 $\mu mol.m^{-2}.s^{-1}$). This phenomena was also reported by
452 Paasche (1999) and Zondervan et al. (2002). Several other studies reported as well similar variations with *E.*
453 *huxleyi* but different strains: Rokitta and Rost (2012) found a decrease of PIC:POC ratio between 50 and 300
454 $\mu mol.m^{-2}.s^{-1}$ for a comparable pCO_2 as our experiments; same observations for Feng et al. (2008) who
455 reported also a decreasing ratio between 50 and 400 $\mu mol.m^{-2}.s^{-1}$; the light intensities experiments of
456 Trimborn et al. (2007) showed a decrease of the ratio with a decreasing light from 300 to 30 $\mu mol.m^{-2}.s^{-1}$;
457 and Rost et al. (2002) found an increase of the PIC:POC ratio between 15, 30 and 80 $\mu mol.m^{-2}.s^{-1}$, again for a
458 comparable pCO_2 as our experiments, and then a decrease of the ratio from 80 to 150 $\mu mol.m^{-2}.s^{-1}$. Our
459 results indicate that calcification was already more severely limited than photosynthesis at 30 $\mu mol.m^{-2}.s^{-1}$
460 in the strain RCC911.
461 The correlations between DSL and coccosphere size (R^2=0.73, p<0.05, n=7) and between DSL and cell size
462 (R^2=0.85, p<0.003, n=7) are illustrated in Fig. 6 and the results are consistent with the correlation reported
463 by Gibbs et al. (2013) between coccoliths and coccospheres in fossil sediment samples. These observations
464 suggest that coccosphere and coccolith size in the water column and in sediments could be used as a proxy
465 for cell size and PIC quota (Aloisi, 2015).
466

467 **4.1.1 Summary effect of nutrient limitation**
468 Apart for the phosphate limited and low light experiment, nutrient limitation slowed down the cell division
469 and so brought the cell into a stationary phase at the end of the experiment. Nutrient limitation as well
470 decreased the particulate organic matter quota corresponding to the limited nutrient (POP for P-limitation
471 and PON for N-limitation) and increased the PIC:POC ratio for both light conditions. The effect of nutrient
472 limitation on morphological properties is more complicated to describe due to large error bar. However, an
473 increase in cell/coccosphere size was observed under P-limitation and almost no effect was reported by the
474 N-limitation.
475

Biogeosciences Discuss., doi:10.5194/bg-2016-196, 2016
Manuscript under review for journal Biogeosciences
Published: 14 June 2016

4.1.2 Summary effect of light limitation

Light limitation decreased the PIC quota and the cell size tended to decrease (no measurement for coccospheres and coccoliths size). PIC:POC ratio decreased with light limitation in every nutrient conditions whereas PON:POC and POP:POC increased with light limitation. As reported by Zondervan (2007), further investigations need to be carried out to improve the understanding of the effect of light intensity on the PIC:POC ratio.

4.1.3 Summary effect of co-limitation

P-limitation induces an important increase in cell size which is less important in low light where cells were able to continue to divide in contrast to the P-limited and high light experiment. These observations support that the cells growth is less affected by the P-limitation in low light than in high light conditions. PIC:POC was higher in N-limited and low light conditions whereas in high light conditions P-limited experiment got the higher ratio.

4.2 E. huxleyi physiological parameters obtained by modelling growth in a batch reactor

The Droop model (Fig. 6 to 8) was able to accurately reproduce the experimental data obtained using *E. huxleyi* strain RCC911 as well as the data of Langer et al. (2013). The Monod model, however, was not able to reproduce the rise in cell number after the limiting nutrient had been exhausted (Fig. 7). This shows that, as for several other phytoplankton groups (Lomas and Glibert, 2000), *E. huxleyi* has the ability to store nutrients internally to continue growth to some extent when external nutrient levels become very low. In our experiments and those of Langer et al. (2013), cells grew on their internal nutrient reserves and managed two to three cell divisions in the absence of external nutrients.

Numerous studies have estimated the maximum nutrient uptake rate V_{max} and the half-saturation constant for nutrient uptake $K_{N/P}$, especially for nitrate uptake, for a variety of phytoplankton species. The values obtained in our study for K_N for high light *E. huxleyi* cultures (Table 4) are comparable to those reported in the literature. Using *E. huxleyi* in chemostat experiments, Riegman et al., (2000) found K_N values between 0.18 and 0.24 µM and K_P between 0.10 and 0.47 µM. In addition, they reported a V_{maxN} of $7.4.10^{-6}$ µmol.cell^{-1}.d^{-1} which is between the V_{maxN} found for PML B92/11 and for RCC911 (Table 4).

When comparing physiological parameters between phytoplankton taxa, the scaling of physiological parameters with cell size has to be taken into account (Marañón et al., 2013).

Marañón et al. (2013) plotted Q_{min} and μ_{max} against cell size (see Fig. 13A for Q_{min} versus cell size) for different phytoplankton species. In these plots coccolithophores fall with the smallest diatoms. Figure 13B reports V_{maxN} versus cell size for different groups of phytoplankton based on the results of Litchman et al. (2007) (using a compiled database) and of Marañón et al. (2013) (22 species cultivated) and the results

Biogeosciences Discuss., doi:10.5194/bg-2016-196, 2016
Manuscript under review for journal Biogeosciences
Published: 14 June 2016

obtained with the Droop model in this study. Despite the different procedures used to obtain V_{maxN} (simulated with a model or measured experimentally), all values for coccolithophores fall in the same range.

Litchman et al. (2007) found a linear correlation between the maximum uptake rate and the half-saturation constant for nitrate uptake as in Collos et al. (2005) across phytoplankton groups (Fig. 14). This correlation defines a physiological trade-off between the capacity to assimilate nutrients efficiently (high V_{max}) and thus grow rapidly, and the capacity to assimilate nutrients in low-nutrient environments (low $K_{N/P}$) and thus thrive in oligotrophic conditions. This analysis shows that large phytoplankton like diatoms and dinoflagellates have high maximum nitrate uptake rates and high half-saturation constant for nitrate uptake. As reported by Cavender-Bares et al. (2001), small cells are mainly found in low nutrient concentration environment whereas larger cells are more abundant in high nutrient environment. *E. huxleyi* maximum uptake rate and half-saturation constant for nitrate uptake were found to be low compared to the other groups and their maximum growth rate is amongst the highest which means that it will be more abundant in low nitrate waters compared to diatoms and dinoflagellates (Litchman et al., 2007). According to Gregg and Casey (2007), there is a high affinity of coccolithophores for low nutrient and low light environments, whereas in high nutrient and high light environments, coccolithophores will be disadvantaged compared to diatoms and cyanobacteria because of their high growth rate and higher sinking rate, respectively. The ideal conditions for an optimal abundance of coccolithophores will be low nutrient and low light areas with a parallel inhibition of the growth of diatoms and chlorophytes, but with vertical mixing strong enough to avoid the sinking of cells (Gregg and Casey, 2007).

The Droop model presented in this paper provides a simple procedure to obtain fundamental physiological parameters from batch culture experiments. Usually physiological parameters are obtained experimentally using continuous laboratory cultures (chemostats) (Eppley and Renger, 1974; Terry, 1982; Riegman et al., 2000; Müller et al., 2012). However, batch cultures are easier to carry out and require minimal equipment and are hence often used for culture experiments (LaRoche et al., 2010).

4.3 Controls on E. huxleyi growth in the deep BIOSOPE niche

The BIOSOPE cruise was carried out in 2004 along a transect across the South Pacific Gyre from the Marquesas Islands to the Peru-Chili upwelling zone. The aim of this expedition was to study the biological, biogeochemical and bio-optical properties (Claustre et al., 2008) of the most oligotrophic zone of the world's ocean (Claustre and Maritorena, 2003). The deep ecological niche of coccolithophores along this transect occurred at the Deep Chlorophyll Maximum (DCM) (Beaufort et al., 2007). According to Claustre et al. (2008) and Raimbault et al. (2007), the nitrate concentration at the GYR station at the deep coccolithophore niche (between 150 and 200m depth) was between 0.01 and 1 µM. In our nitrate-limited

Biogeosciences Discuss., doi:10.5194/bg-2016-196, 2016
Manuscript under review for journal Biogeosciences
Published: 14 June 2016

548 low light culture experiment (Fig. 15), this concentration occurred between the end of the exponential
549 growth phase and the beginning of the stationary phase (days 8 to 9), when nitrate-limitation began to
550 affect instantaneous growth rates. Our phosphate-limited experiment did not proceed long enough for the
551 instantaneous growth rate to decrease appreciably, but Claustre et al. (2008) reported a nitrate
552 concentration <3 nM in the 0-100 m water column and a detectable phosphate concentration always above
553 0.1 µM in surface layers (Raimbault and Garcia, 2008) and Moutin et al. (2008) concluded that phosphate is
554 apparently not the limiting nutrient for phytoplankton along the BIOSOPE transect. The picture that
555 emerges is consistent with the model of Klausmeier and Litchman (2001), who predicted that limitation of
556 growth in a DCM should be limited by both light and one nutrient, with the upper layer of the DCM being
557 limited by nutrient supply and the deeper layer by light. However, the vertical diffusivity of nitrate through
558 the nitracline needs to take into account and could potentially bring dissolved nitrate into the deep niche of
559 coccolithophores (Holligan et al., 1984). The experiments and modelling work presented here allow us to
560 conclude that the growth of *E. huxleyi* in the deep ecological niche at the GYR station of the BIOSOPE
561 transect is clearly limited by the light and potentially limited by the dissolved nitrate, with *E. huxleyi* growth
562 in the upper part of the niche mostly co-limited by irradiance intensity and nitrate availability, whereas
563 irradiance is the main limiting factor in the lower part of the niche where nitrate becomes more
564 concentrated.
565 The depth-distribution of the modelled *E. huxleyi* growth rate, and of dissolved nitrogen, light intensity,
566 chlorophyll a concentration and coccolithophore abundance supports the inferred light-nitrate co-
567 limitation (Fig. 16). We used the physiological parameters constrained in our experiments together with a
568 steady state assumption for uptake and assimilation of nitrate (see appendix) to obtain the vertical profile
569 of *E. huxleyi* growth rate at the GYR station (Fig. 16). This calculation, forced by the irradiance and nitrate
570 data at the GYR station, shows that *E. huxleyi* growth rate is maximal at the depth of the maximum
571 chlorophyll a concentration. The half-saturation constant for nitrate uptake K_N constrained with the Droop
572 model (0.09 µmol.L^{-1}) lies within the deep niche (Fig. 16). The maximum growth rate at the GYR station
573 (0.024 d^{-1} at 175 m depth) corresponds to an *E. huxleyi* generation time of 29.28 days, suggesting that
574 division rate at the DCM is very slow (so slow that it would be difficult to reproduce in culture experiments).
575 This point highlights the importance of this growth rate calculation which provides a useful way to
576 investigate the growth potential of *E. huxleyi* in the DCM of the South Pacific Gyre. Moreover, as the growth
577 rate for the low light culture and replete conditions experiments was at 0.28 d^{-1} with an irradiance of
578 approximately 30 µmol.m^{-2}.s^{-1}, it is not surprising that the potential growth rate in the deep niche was so
579 small at irradiance below 20 µmol.m^{-2}.s^{-1} and low nitrate concentration.
580 With the above limitation pattern in mind, it is possible to predict the effect of nitrate and light variability
581 on the vertical changes in the *E. huxleyi* PIC:POC ratio in gyre conditions. According to our experimental
582 results, the PIC:POC ratio increases slightly with nitrate limitation but the strongest effect on PIC:POC ratio
583 seems to be supported by light intensity. As explain in the Sect. 4.1 of this discussion, several studies have

Biogeosciences Discuss., doi:10.5194/bg-2016-196, 2016
Manuscript under review for journal Biogeosciences
Published: 14 June 2016

584 shown that the ratio increases with light decreasing above a range of light between 30 and 80 µmol.m^{-2}.s^{-1}
585 but decreases with a light limitation below this range. Considering Fig. 16, the PIC:POC ratio in *E. huxleyi*
586 would be expected to be intermediate in surface waters (nitrate-poor but strongly high light intensity;
587 approximately 1800 µmol.m^{-2}.s^{-1}), then increases to attain a maximum value between the lower part of
588 subsurface waters and the beginning of the deep niche (between 80 µmol.m^{-2}.s^{-1} and 30 µmol.m^{-2}.s^{-1} ;
589 therefore between 110 m and 150 m depth), decrease in the lower part of the deep niche, and finally
590 decreases drastically in deeper water, nitrate-rich but low-irradiance waters. This prediction cannot be
591 verified with the available published data from the BIOSOPE transect, but same conclusions for the upper
592 part of the ocean have been observed through in situ measurements by Fernández et al. (1993) and these
593 predictions could easily be verified in future expeditions to coccolithophore-bearing DCM zones.
594 Klaas and Archer (2002) reported that calcium carbonate is mainly exported by coccolithophores to the
595 deep sea and that the rain of organic carbon is mostly conducted by calcium carbonate because of its
596 higher density than opal and higher abundance than terrigenous material. Then a decrease of PIC quota by
597 low irradiance will decrease the calcium carbonate rain to the sediments related to *E. huxleyi.* However, the
598 cellular PIC quota is maybe decreasing but the PIC total increase in the deep niche compared to the upper
599 and deeper water column. In this context the effect on rain ratio, therefore on carbon pump and carbonate
600 counter-pump, needs to be integrated over the whole photic zone and considering the whole particulate
601 organic and inorganic matter.

602 ## 5. Concluding remarks
603
604 We present one of the few laboratory cultures experiments investigating the growth and PIC:POC ratio of
605 the coccolithophore *E. huxleyi* in light- and nutrient-limited conditions, mimicking those of the deep
606 ecological niche of coccolithophores of the South Pacific Gyre (Beaufort et al., 2007; Claustre et al., 2008).
607 By combining batch culture experiments with a simple numerical model based on the internal stores
608 (Droop) concept, we show that: 1) *E. huxleyi* has the capacity to divide up to three times in the absence of
609 external nutrients by using internal nutrient stores and is more affected by phosphate limitation in high
610 light than in low light conditions; 2) a simple batch culture experimental set-up, as opposed to the more
611 time-consuming and expensive continuous culture approach, can be used to obtain fundamental
612 physiological parameters, such as the maximum surface- normalized nutrient uptake rate and the half-
613 saturation constant for nutrient uptake, that describe the response of phytoplankton growth to
614 environmental conditions; 3) the position of the deep coccolithophore niche of the South Pacific Gyre was
615 defined by the maximum of coccosphere reported by Beaufort et al. (2007) and the limitation of growth in
616 this niche is the result of contrasting gradients of light (decreasing downwards) and nitrate (decreasing
617 upwards), studied through a combination of experimental results, Droop modelling and in situ data; and
618 confirming the theoretical prediction of Klausmeier and Litchman (2001).

Biogeosciences Discuss., doi:10.5194/bg-2016-196, 2016
Manuscript under review for journal Biogeosciences
Published: 14 June 2016

Appendix

To obtain the growth rate through the vertical profile at the station GYR, we needed to express the cellular quota Q_N of a function of the nitrate concentration NO_3 *[N].* To deal with this purpose, we resolve the system of three equations from the Droop theory:

$$\frac{dQ_N}{dt} = N_{up} - \mu \cdot Q_N \quad \text{(A1)}$$

$$N_{up} = S_{cell} \cdot V_{\max} \cdot \frac{[N]}{[N] + K_N} \quad \text{(A2)}$$

$$\mu = \mu_{\max} \cdot \frac{(1+KQ)\cdot(Q - Q_N^{\min})}{(Q - Q_N^{\min}) + KQ \cdot (Q_N^{\max} - Q_N^{\min})} \quad \text{(A3)}$$

Considering a stationary state (uptake-assimilation steady state) and thus assuming the differential Eq. (A1) equal to zero, we resolve the system to express the cellular quota Q_N versus the nitrate concentration (see Fig. A1):

$$A = \frac{1}{2\cdot(1+KQ)\cdot\mu_{\max}\cdot(K_N + [N])} \cdot \left((K_N \cdot (1+KQ)\cdot\mu_{\max}\cdot Q_N^{\min}) \right) \quad \text{(A4)}$$

$$B = \left((1+KQ)\cdot\mu_{\max}\cdot[N]\cdot Q_N^{\min} \right) + \left([N]\cdot S_{cell}\cdot V_{\max} \right) \quad \text{(A5)}$$

$$C = \sqrt{\begin{array}{l} 4(1+KQ)\cdot\mu_{\max}\cdot[N]\cdot(K_N+[N])\cdot(KQ\cdot Q_N^{\max} - (1+KQ)\cdot Q_N^{\min})\cdot S_{cell}\cdot V_{\max} \\ + \left((1+KQ)\cdot\mu_{\max}\cdot(K_N+[N])\cdot Q_N^{\min} + [N]\cdot S_{cell}\cdot V_{\max} \right)^2 \end{array}} \quad \text{(A6)}$$

$$Q_N = A + B + C \quad \text{(A7)}$$

Thus, the growth rate can be express depending of the irradiance (and *KIrr*; see Sect. 2.2.1) and the cellular quota Q_N. The other parameters are known (output of the model for the experiment reproducing the condition of the nitracline):

$$\mu = \mu_{\max} \cdot \frac{(1+KQ)\cdot(Q - Q_N^{\min})}{(Q - Q_N^{\min}) + KQ \cdot (Q_N^{\max} - Q_N^{\min})} \cdot \frac{Irr}{Irr + KIrr} \quad \text{(A8)}$$

Biogeosciences Discuss., doi:10.5194/bg-2016-196, 2016
Manuscript under review for journal Biogeosciences
Published: 14 June 2016

The vertical profile of the growth rate of coccolithophores at the station GYR, calculated with the previous equation, is shown in the Fig. 16.

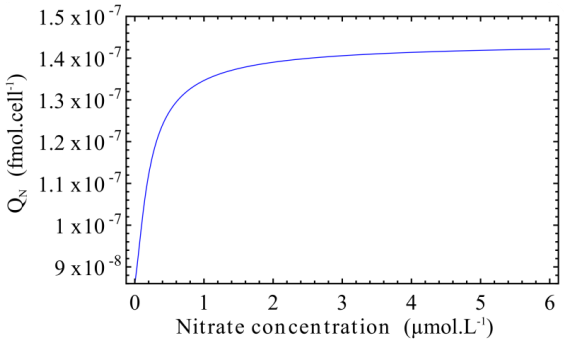

Figure A1. Cellular quota of nitrogen versus the nitrate concentration using parameters of the best-fit results of the model ran for the low light and nitrate limited experiment with RCC911.

Acknowledegements

This project was supported by the TELLUS CLIMAHUX project (INSU-CNRS) and the MODIF project of the Institut Pierre Simon Laplace (IPSL). We thanks C. Schmechtig for having provide access to the BIOSOPE data base, F. Le cornec and I. Djouraev for helping with the PIC analysis at the Institut de Recherche pour le Développement (IRD) ALYSE platform and C. Labry and A. Youenou for carrying out the POP analysis at IFREMER. We are grateful to C. Leroux for the analysis of our POC, PON samples and the research team CHIM from the Station Biologique of Roscoff for their help: T. Cariou for the dissolved nutrients analysis and de-carbonatation of the POC, PON samples; M. Vernet for help processing DIC samples; and Y. Bozec for DIC analysis. We thank as well A. Charantonis for his statistical advices for the modelling part. The lead author is supported by a doctoral fellowship from the French Minister of Education and Research (MESR).

Biogeosciences Discuss., doi:10.5194/bg-2016-196, 2016
Manuscript under review for journal Biogeosciences
Published: 14 June 2016

675 **References**

676

677 Aloisi, G.: Co-variation of metabolic rates and cell-size in coccolithophores, Biogeosciences Discuss, 12,
678 6215–6284, doi:doi:10.5194/bgd-12-6215-2015, 2015.

679 Beaufort, L., Couapel, M., Buchet, N. and Claustre, H.: Calcite production by Coccolithophores in the South
680 East Pacific Ocean: from desert to jungle, Biogeosciences Discuss, 4(5), 3267–3299, doi:10.5194/bgd-4-
681 3267-2007, 2007.

682 Berry, L., Taylor, A. R., Lucken, U., Ryan, K. P. and Brownlee, C.: Calcification and inorganic carbon
683 acquisition in coccolithophores, Funct. Plant Biol., 29(3), 289–299, doi:doi:10.1071/PP01218, 2002.

684 van Bleijswijk, J. D. L., Kempers, R. S., Veldhuis, M. J. and Westbroek, P.: Cell and Growth Characteristics of
685 Types a and B of Emiliania Huxleyi (prymnesiophyceae) as Determined by Flow Cytometry and Chemical
686 Analyses1, J. Phycol., 30(2), 230–241, doi:10.1111/j.0022-3646.1994.00230.x, 1994.

687 Boyd, P. W., Strzepek, R., Fu, F. and Hutchins, D. A.: Environmental control of open-ocean phytoplankton
688 groups: Now and in the future, Limnol. Oceanogr., 55(3), 1353–1376, doi:10.4319/lo.2010.55.3.1353, 2010.

689 Buitenhuis: Growth rates of six coccolithophorid strains as a function of temperature, Limnol. Oceanogr.,
690 53(3), 1181–1185, doi:10.4319/lo.2008.53.3.1181, 2008.

691 Cavender-Bares, K. K., Karl, D. M. and Chisholm, S. W.: Nutrient gradients in the western North Atlantic
692 Ocean: Relationship to microbial community structure and comparison to patterns in the Pacific Ocean,
693 Deep Sea Res. Part Oceanogr. Res. Pap., 48(11), 2373–2395, doi:10.1016/S0967-0637(01)00027-9, 2001.

694 Claustre, H. and Maritorena, S.: The Many Shades of Ocean Blue, , 302(5650), 1514–1515, 2003.

695 Claustre, H., Sciandra, A. and Vaulot, D.: Introduction to the special section bio-optical and biogeochemical
696 conditions in the South East Pacific in late 2004: the BIOSOPE program, Biogeosciences, 5(3), 679–691,
697 doi:10.5194/bg-5-679-2008, 2008.

698 Cortés, M. Y., Bollmann, J. and Thierstein, H. R.: Coccolithophore ecology at the HOT station ALOHA, Hawaii,
699 Deep Sea Res. Part II Top. Stud. Oceanogr., 48(8–9), 1957–1981, doi:10.1016/S0967-0645(00)00165-X,
700 2001.

701 Daniels, C. J., Sheward, R. M. and Poulton, A. J.: Biogeochemical implications of comparative growth rates
702 of Emiliania huxleyi and Coccolithus species, Biogeosciences, 11(23), 6915–6925, doi:10.5194/bg-11-6915-
703 2014, 2014.

704 Droop, M. R.: Vitamin B12 and Marine Ecology. IV. The Kinetics of Uptake, Growth and Inhibition in
705 Monochrysis Lutheri, J. Mar. Biol. Assoc. U. K., 48(3), 689–733, doi:10.1017/S0025315400019238, 1968.

706 Engel, A., Cisternas Novoa, C., Wurst, M., Endres, S., Tang, T., Schartau, M. and Lee, C.: No detectable effect
707 of CO2 on elemental stoichiometry of Emiliania huxleyi in nutrient-limited, acclimated continuous cultures,
708 Mar. Ecol. Prog. Ser., 507, 15–30, doi:10.3354/meps10824, 2014.

709 Eppley, R. W. and Renger, E. H.: Nitrogen Assimilation of an Oceanic Diatom in Nitrogen-Limited Continuous
710 Culture, J. Phycol., 10(1), 15–23, doi:10.1111/j.1529-8817.1974.tb02671.x, 1974.

711 Feng, Y., Warner, M. E., Zhang, Y., Sun, J., Fu, F.-X., Rose, J. M. and Hutchins, D. A.: Interactive effects of
712 increased pCO2, temperature and irradiance on the marine coccolithophore Emiliania huxleyi
713 (Prymnesiophyceae), Eur. J. Phycol., 43(1), 87–98, doi:10.1080/09670260701664674, 2008.

714 Fernández, E., Boyd, P., Holligan, P. M. and Harbour: Production of organic and inorganic carbon within a
715 large-scale coccolithophore bloom in the northeast Atlantic Ocean, Mar. Ecol. Prog. Ser., 97, 271–285,
716 1993.

717 Flynn, K.: The importance of the form of the quota curve and control of non-limiting nutrient transport in
718 phytoplankton models, J. Plankton Res., 30(4), 423–438, doi:10.1093/plankt/fbn007, 2008.

719 Follows, M. J. and Dutkiewicz, S.: Modeling Diverse Communities of Marine Microbes, Annu. Rev. Mar. Sci.,
720 3(1), 427–451, doi:10.1146/annurev-marine-120709-142848, 2011.

721 Fritz, J. J.: Carbon fixation and coccolith detachment in the coccolithophore Emiliania huxleyi in nitrate-
722 limited cyclostats, Mar. Biol., 133(3), 509–518, doi:10.1007/s002270050491, 1999.

723 Gibbs, S. J., Poulton, A. J., Brown, P. R., Daniels, C. J., Hopkins, J., Young, J. R., Jones, H. L., Thiemann, G. J.,
724 O'Dea, S. A. and Newsam, C.: Species-specific growth response of coccolithophores to Palaeocene–Eocene
725 environmental change, Nat. Geosci., 6, 218–222, doi:10.1038/NGEO1719, 2013.

726 Gregg, W. W. and Casey, N. W.: Modeling coccolithophores in the global oceans, Deep Sea Res. Part II Top.
727 Stud. Oceanogr., 54(5–7), 447–477, doi:10.1016/j.dsr2.2006.12.007, 2007.

728 Haidar, A. T. and Thierstein, H. R.: Coccolithophore dynamics off Bermuda (N. Atlantic), Deep Sea Res. Part
729 II Top. Stud. Oceanogr., 48(8–9), 1925–1956, doi:10.1016/S0967-0645(00)00169-7, 2001.

730 Henderiks, J., Winter, A., Elbrchter, M., Feistel, R., Plas, A. van der, Nausch, G. and Barlow, R.:
731 Environmental controls on Emiliania huxleyi morphotypes in the Benguela coastal upwelling system (SE
732 Atlantic), Mar. Ecol. Prog. Ser., 448, 51–66, doi:10.3354/meps09535, 2012.

733 Holligan, P. M., Balch, W. M. and Yentsch, C. M.: The significance of subsurface chlorophyll, nitrite and
734 ammonium maxima in relation to nitrogen for phytoplankton growth in stratified waters of the Gulf of
735 Maine, J. Mar. Res., 42(4), 1051–1073, doi:10.1357/002224084788520747, 1984.

736 Holligan, P. M., Fernández, E., Aiken, J., Balch, W. M., Boyd, P., Burkill, P. H., Finch, M., Groom, S. B., Malin,
737 G., Muller, K., Purdie, D. A., Robinson, C., Trees, C. C., Turner, S. M. and van der Wal, P.: A biogeochemical
738 study of the coccolithophore, Emiliania huxleyi, in the North Atlantic, Glob. Biogeochem. Cycles, 7(4), 879–
739 900, doi:10.1029/93GB01731, 1993.

740 Iglesias-Rodriguez, M. D., Halloran, P. R., Rickaby, R. E. M., Hall, I. R., Colmenero-Hidalgo, E., Gittins, J. R.,
741 Green, D. R. H., Tyrrell, T., Gibbs, S. J., von Dassow, P., Rehm, E., Armbrust, E. V. and Boessenkool, K. P.:
742 Phytoplankton calcification in a high-CO2 world, Science, 320(5874), 336–340,
743 doi:10.1126/science.1154122, 2008.

744 Jordan, R. W. and Winter, A.: Assemblages of coccolithophorids and other living microplankton off the coast
745 of Puerto Rico during January–May 1995, Mar. Micropaleontol., 39(1–4), 113–130, doi:10.1016/S0377-
746 8398(00)00017-7, 2000.

747 Kaffes, A.: Carbon and nitrogen fluxes in the marine coccolithophore Emiliania huxleyi grown under
748 different nitrate concentrations, J. Exp. Mar. Biol. Ecol., 393, 1–8, doi:10.1016/j.jembe.2010.06.004, 2010.

749 Keller, M., Selvin, R., Claus, W. and Guillard, R.: Media for the culture of oceanic ultraphytoplankton, J.
750 Phycol., 23, 633–638, 1987.

751 Klaas, C. and Archer, D. E.: Association of sinking organic matter with various types of mineral ballast in the
752 deep sea: Implications for the rain ratio, Glob. Biogeochem. Cycles, 16(4), 1116,
753 doi:10.1029/2001GB001765, 2002.

754 Klausmeier, C. A. and Litchman, E.: Algal games: The vertical distribution of phytoplankton in poorly mixed
755 water columns, Limnol Ocean., 46(8), 1998–2007, 2001.

756 Krug, S. A., Schulz, K. G. and Riebesell, U.: Effects of changes in carbonate chemistry speciation on
757 Coccolithus braarudii: a discussion of coccolithophorid sensitivities, Biogeosciences, 8(3), 771–777,
758 doi:10.5194/bg-8-771-2011, 2011.

759 Labry, C., Youenou, A., Delmas, D. and Michelon, P.: Addressing the measurement of particulate organic
760 and inorganic phosphorus in estuarine and coastal waters, Cont. Shelf Res., 60, 28–37,
761 doi:10.1016/j.csr.2013.04.019, 2013.

762 Langer, G., Geisen, M., Baumann, K.-H., Kläs, J., Riebesell, U., Thoms, S. and Young, J. R.: Species-specific
763 responses of calcifying algae to changing seawater carbonate chemistry, Geochem. Geophys. Geosystems,
764 7(9), 155–161, doi:10.1029/2005GC001227, 2006.

765 Langer, G., Gussone, N., Nehrke, G., Riebesell, U., Eisenhauer, A. and Thoms, S.: Calcium isotope
766 fractionation during coccolith formation in Emiliania huxleyi: Independence of growth and calcification rate,
767 Geochem. Geophys. Geosystems, 8(5), Q05007, doi:10.1029/2006GC001422, 2007.

768 Langer, G., Oetjen, K. and Brenneis, T.: Calcification of Calcidiscus leptoporus under nitrogen and
769 phosphorus limitation, J. Exp. Mar. Biol. Ecol., 413, 131–137, doi:10.1016/j.jembe.2011.11.028, 2012.

770 Langer, G., Oetjen, K. and Brenneis, T.: Coccolithophores do not increase particulate carbon production
771 under nutrient limitation: A case study using Emiliania huxleyi (PML B92/11), J. Exp. Mar. Biol. Ecol., 443,
772 155–161, doi:10.1016/j.jembe.2013.02.040, 2013.

773 LaRoche, J., Rost, B. and Engel, A.: Bioassays, batch culture and chemostat experimentation, Riebesell, U.,
774 Fabry, V.J., Hansson, L., Gattuso, J.-P. (Eds.), Guide to Best Practices for Ocean Acidification Research and
775 Data Reporting. Publications Office of the European Union., 2010.

776 Leonardos, N. and Geider, R. J.: Elevated atmospheric carbon dioxide increases organic carbon fixation by
777 Emiliania huhleyi (Haptophyta), under nutrient-limited high-light conditions., J. Phycol., 41(6), 1196–1203,
778 doi:10.1111/j.1529-8817.2005.00152.x, 2005.

779 Litchman, E., Klausmeier, C. A., Schofield, O. M. and Falkowski, P. G.: The role of functional traits and trade-
780 offs in structuring phytoplankton communities: scaling from cellular to ecosystem level, Ecol. Lett., 10(12),
781 1170–1181, doi:10.1111/j.1461-0248.2007.01117.x, 2007.

782 Loisel, H., Nicolas, J.-M., Sciandra, A., Stramski, D. and Poteau, A.: Spectral dependency of optical
783 backscattering by marine particles from satellite remote sensing of the global ocean, J. Geophys. Res.,
784 111(C09024), doi:10.1029/2005JC003367, 2006.

785 Lomas, M. W. and Glibert, P. M.: Comparisons of Nitrate Uptake, Storage, and Reduction in Marine Diatoms
786 and Flagellates, J. Phycol., 36(5), 903–913, doi:10.1046/j.1529-8817.2000.99029.x, 2000.

787 MacIntyre, H. L., Kana, T. M., Anning, T. and Geider, R. J.: Photoacclimation of Photosynthesis Irradiance
788 Response Curves and Photosynthetic Pigments in Microalgae and Cyanobacteria1, J. Phycol., 38(1), 17–38,
789 doi:10.1046/j.1529-8817.2002.00094.x, 2002.

790 Marañón, E., Cermeño, P., López-Sandoval, D. C., Rodríguez-Ramos, T., Sobrino, C., Huete-Ortega, M.,
791 Blanco, J. M. and Rodríguez, J.: Unimodal size scaling of phytoplankton growth and the size dependence of
792 nutrient uptake and use, Ecol. Lett., 16(3), 371–379, doi:10.1111/ele.12052, 2013.

793 Monod, J.: The Growth of Bacterial Cultures., Annual Review of Microbiology., 1949.

794 Morel, A., Gentili, B., Claustre, H., Babin, M., Bricaud, A., Ras, J. and Tièche, F.: Optical properties of the
795 "clearest" natural waters, Limnol. Oceanogr., 52(1), 217–229, doi:10.4319/lo.2007.52.1.0217, 2007.

796 Moutin, T., Karl, D. M., Duhamel, S., Rimmelin, P., Raimbault, P., Van Mooy, B. A. S. and Claustre, H.:
797 Phosphate availability and the ultimate control of new nitrogen input by nitrogen fixation in the tropical
798 Pacific Ocean, Biogeosciences, 5(1), 95–109, doi:10.5194/bg-5-95-2008, 2008.

799 Müller, M. N., Antia, A. N. and LaRoche, J.: Influence of cell cycle phase on calcification in the
800 coccolithophore Emiliania huxleyi, Limnol. Oceanogr., 53(2), 506–512, doi:10.4319/lo.2008.53.2.0506,
801 2008.

802 Müller, M. N., Beaufort, L., Bernard, O., Pedrotti, M. L., Talec, A. and Sciandra, A.: Influence of CO2 and
803 nitrogen limitation on the coccolith volume of Emiliania huxleyi (Haptophyta), Biogeosciences, 9(10), 4155–
804 4167, doi:10.5194/bg-9-4155-2012, 2012.

805 Okada, H. and McIntyre, A.: Seasonal distribution of modern coccolithophores in the western North Atlantic
806 Ocean, Mar. Biol., 54(4), 319–328, doi:10.1007/BF00395438, 1979.

807 Oviedo, A. M., Langer, G. and Ziveri, P.: Effect of phosphorus limitation on coccolith morphology and
808 element ratios in Mediterranean strains of the coccolithophore Emiliania huxleyi, J. Exp. Mar. Biol. Ecol.,
809 459, 105–113, 2014.

810 Paasche, E.: Roles of nitrogen and phosphorus in coccolith formation in Emiliania huxleyi
811 (Prymnesiophyceae), Eur. J. Phycol., 33(1), 33–42, doi:10.1080/09670269810001736513, 1998.

812 Paasche, E.: Reduced coccolith calcite production under light-limited growth: a comparative study of three
813 clones of Emiliania huxleyi (Prymnesiophyceae), Phycologia, 38(6), 508–516, doi:10.2216/i0031-8884-38-6-
814 508.1, 1999.

815 Paasche, E.: A review of the coccolithophorid Emiliania huxleyi (Prymnesiophyceae), with particular
816 reference to growth, coccolith formation, and calcification-photosynthesis interactions, Phycologia, 40(6),
817 503–529, doi:10.2216/i0031-8884-40-6-503.1, 2001.

818 Poulton, A. J., Stinchcombe, M. C., Achterberg, E. P., Bakker, D. C. E., Dumousseaud, C., Lawson, H. E., Lee,
819 G. A., Richier, S., Suggett, D. J. and Young, J. R.: Coccolithophores on the north-west European shelf:
820 calcification rates and environmental controls, Biogeosciences, 11(14), 3919–3940, doi:10.5194/bg-11-
821 3919-2014, 2014.

822 Raimbault, P. and Garcia, N.: Evidence for efficient regenerated production and dinitrogen fixation in
823 nitrogen-deficient waters of the South Pacific Ocean: impact on new and export production estimates,
824 Biogeosciences, 5, 323–338, doi:10.5194/bg-5-323-2008, 2008.

825 Raimbault, P., Garcia, N. and Cerutti, F.: Distribution of inorganic and organic nutrients in the South Pacific
826 Ocean – evidence for long-term accumulation of organic matter in nitrogen-depleted waters,
827 Biogeosciences Discuss., 4(4), 3041–3087, 2007.

828 Raven, J. A. and Crawfurd, K.: Environmental controls on coccolithophore calcification, Mar Ecol Prog Ser,
829 470, 137–166, doi:10.3354/meps09993, 2012.

830 Redfield, A. C.: The influence of organisms on the composition of sea-water, The Sea, 26–77, 1963.

831 Riegman, R., Stolte, W., Noordeloos, A. A. M. and Slezak, D.: Nutrient uptake and alkaline phosphatase (ec
832 3:1:3:1) activity of Emiliania huxleyi (PRYMNESIOPHYCEAE) during growth under N and P limitation in
833 continuous cultures, J. Phycol., 36(1), 87–96, doi:10.1046/j.1529-8817.2000.99023.x, 2000.

834 Rokitta, S. D. and Rost, B.: Effects of CO2 and their modulation by light in the life-cycle stages of the
835 coccolithophore Emiliania huxleyi, Limnol. Oceanogr., 57(2), 607–618, 2012.

836 Rost, B., Zondervan, I. and Riebesell, U.: Light-dependent carbon isotope fractionation in the
837 coccolithophorid Emiliania huxleyi, 2002.

838 Rouco, M., Branson, O., Lebrato, M. and Iglesias-Rodríguez, M. D.: The effect of nitrate and phosphate
839 availability on Emiliania huxleyi (NZEH) physiology under different CO2 scenarios, Front. Aquat. Microbiol.,
840 4, 155, doi:10.3389/fmicb.2013.00155, 2013.

841 Sciandra, A., Harlay, J., Lefvre, D., Leme, R., Rimmelin, P., Denis, M. and Gattuso, J.: Response of
842 coccolithophorid Emiliania huxleyi to elevated partial pressure of CO2 under nitrogen limitation, Mar. Ecol.
843 Prog. Ser., 261, 111–122, doi:10.3354/meps261111, 2003.

844 Shutler, J. D., Land, P. E., Brown, C. W., Findlay, H. S., Donlon, C. J., Medland, M., Snooke, R. and Blackford,
845 J. C.: Coccolithophore surface distributions in the North Atlantic and their modulation of the air-sea flux of
846 CO2 from 10 years of satellite Earth observation data, Biogeosciences, 10(4), 2699–2709, doi:10.5194/bg-
847 10-2699-2013, 2013.

848 Terry, K. L.: Nitrate and Phosphate Uptake Interactions in a Marine Prymnesiophyte1, J. Phycol., 18(1), 79–
849 86, doi:10.1111/j.1529-8817.1982.tb03159.x, 1982.

850 Trimborn, S., Langer, G. and Rost, B.: Effect of varying calcium concentrations and light intensities on
851 calcification and photosynthesis in Emiliania huxleyi, Limnol. Oceanogr., 52(5), 2285–2293,
852 doi:10.4319/lo.2007.52.5.2285, 2007.

853 Westbroek, P., Brown, C. W., Bleijswijk, J. van, Brownlee, C., Brummer, G. J., Conte, M., Egge, J., Fernández,
854 E., Jordan, R., Knappertsbusch, M., Stefels, J., Veldhuis, M., van der Wal, P. and Young, J.: A model system
855 approach to biological climate forcing. The example of Emiliania huxleyi, Glob. Planet. Change, 8(1–2), 27–
856 46, doi:10.1016/0921-8181(93)90061-R, 1993.

857 Winter, A. and Siesser: Atlas of living coccolithophores, in Coccolithophores, pp. 107–159, Cambridge.,
858 1994.

859 Winter, A., Henderiks, J., Beaufort, L., Rickaby, R. E. M. and Brown, C. W.: Poleward expansion of the
860 coccolithophore Emiliania huxleyi, J. Plankton Res., 36(2), 316–325, doi:10.1093/plankt/fbt110, 2014.

861 Young, J. R., Poulton, A. J. and Tyrrell, T.: Morphology of Emiliania huxleyi coccoliths on the North West
862 European shelf – is there an influence of carbonate chemistry?, Biogeosciences Discuss, 11(3), 4531–4561,
863 doi:10.5194/bgd-11-4531-2014, 2014.

864 Zondervan, I.: The effects of light, macronutrients, trace metals and CO2 on the production of calcium
865 carbonate and organic carbon in coccolithophores—A review, Deep Sea Res. Part II Top. Stud. Oceanogr.,
866 54(5–7), 521–537, doi:10.1016/j.dsr2.2006.12.004, 2007.

867 Zondervan, I., Rost, B. and Riebesell, U.: Effect of CO2 concentration on the PIC/POC ratio in the
868 coccolithophore Emiliania huxleyi grown under light-limiting conditions and different daylengths, J. Exp.
869 Mar. Biol. Ecol., 272(1), 55–70, doi:10.1016/S0022-0981(02)00037-0, 2002.

870
871
872
873
874
875

Biogeosciences Discuss., doi:10.5194/bg-2016-196, 2016
Manuscript under review for journal Biogeosciences
Published: 14 June 2016

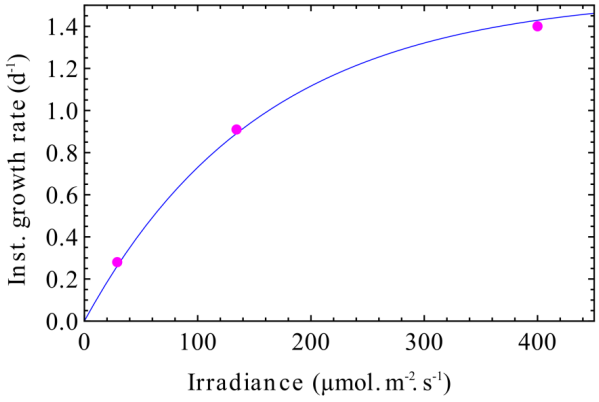

Figure 1. Instantaneous growth rate versus irradiance calculated with equation 9 (*KIrr* = 157 µmol.m^{-2}.s^{-1}). Pink points represent the irradiance and growth rate of the experiments carried out by Langer et al. (2013) and our experiments. The blue line is the result of equation 9.

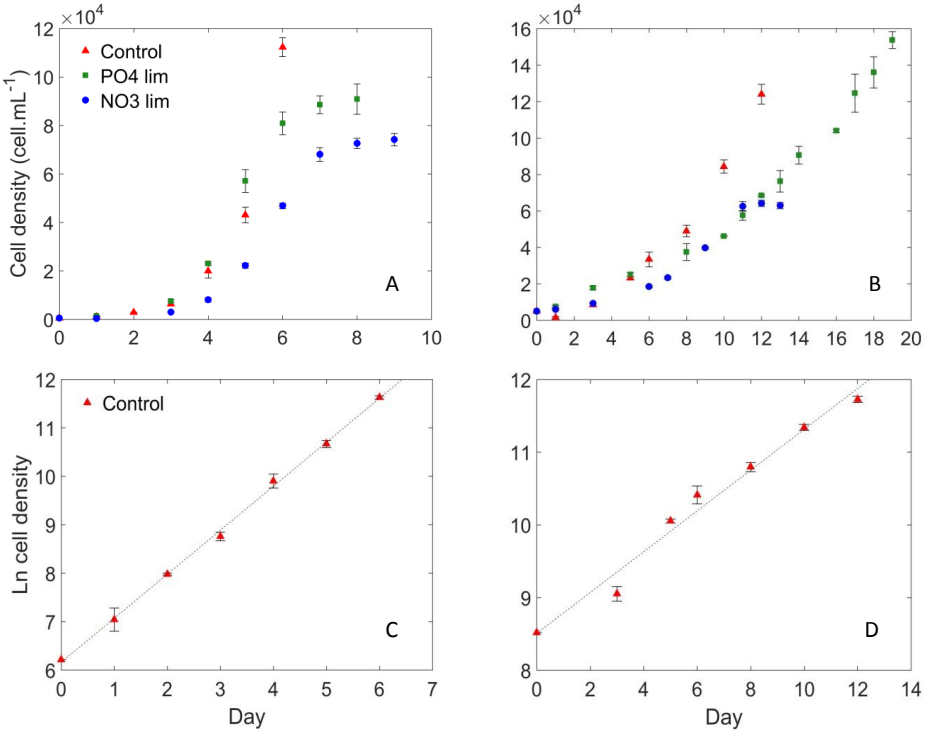

Figure 2. The evolution of cell density with time in culture experiments with *E. huxleyi* strain RCC911 (A: high irradiance; B: low irradiance) and cell density on a logarithmic scale for nutrient-replete cultures (C: high irradiance; D: low irradiance).

Biogeosciences Discuss., doi:10.5194/bg-2016-196, 2016
Manuscript under review for journal Biogeosciences
Published: 14 June 2016

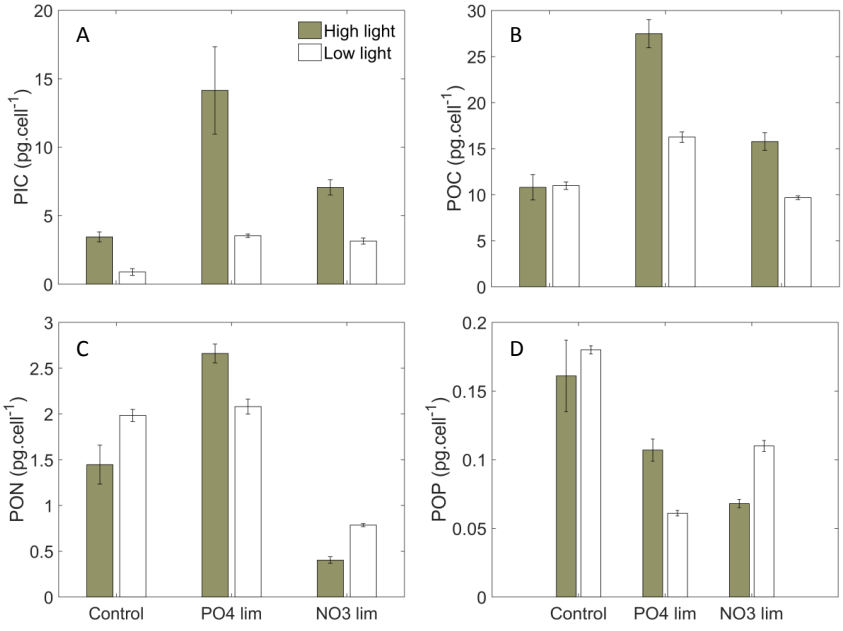

Figure 3. Cellular PIC, POC, PON, POP quotas.

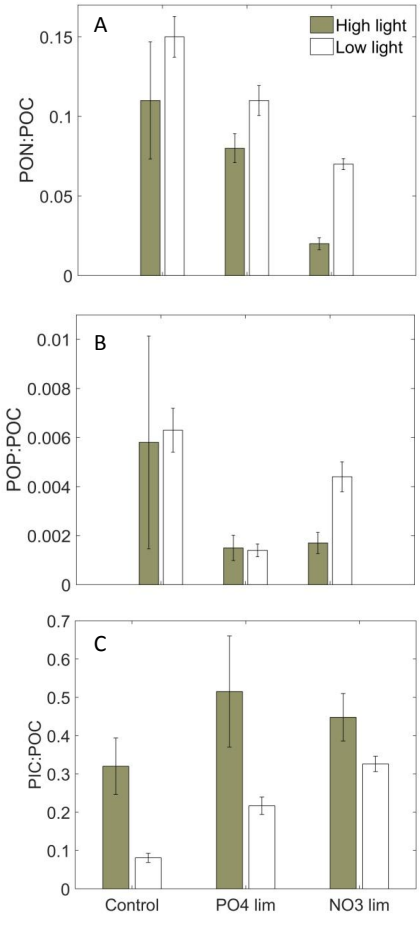

Figure 4. Cellular PON/POC, POP/POC and PIC/POC ratios.

Biogeosciences Discuss., doi:10.5194/bg-2016-196, 2016
Manuscript under review for journal Biogeosciences
Published: 14 June 2016

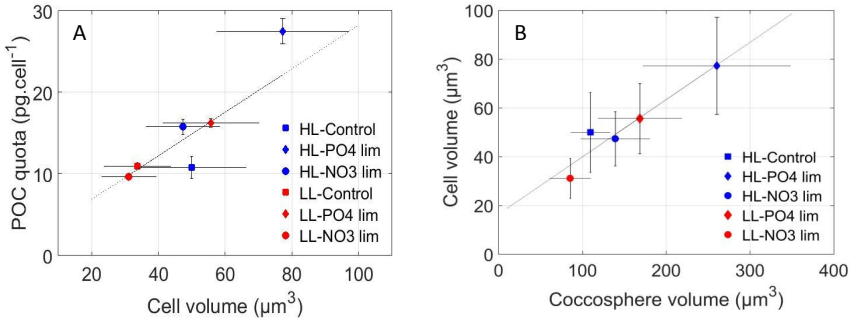

Figure 5. A: POC quota versus cell volume and B: cell volume against coccosphere volume in high light (HL) and low light conditions (LL).

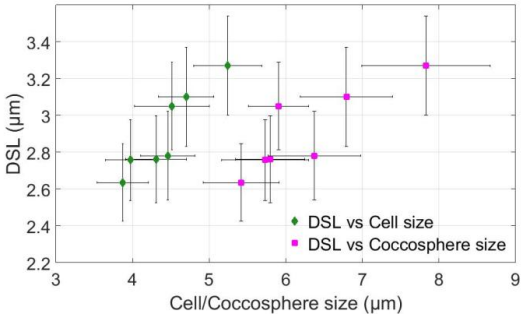

Figure 6. Distal shield length (DSL) versus coccosphere and cell diameter.

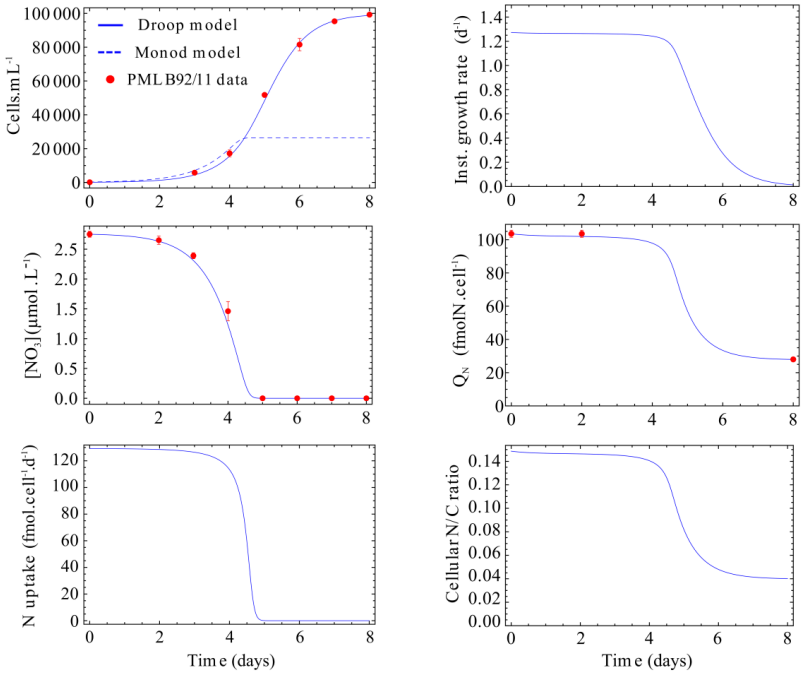

Figure 7. Model fitted to the data of the nitrate-limited cultures of Langer et al. (2013) (Inst = instantaneous)

Biogeosciences Discuss., doi:10.5194/bg-2016-196, 2016
Manuscript under review for journal Biogeosciences
Published: 14 June 2016

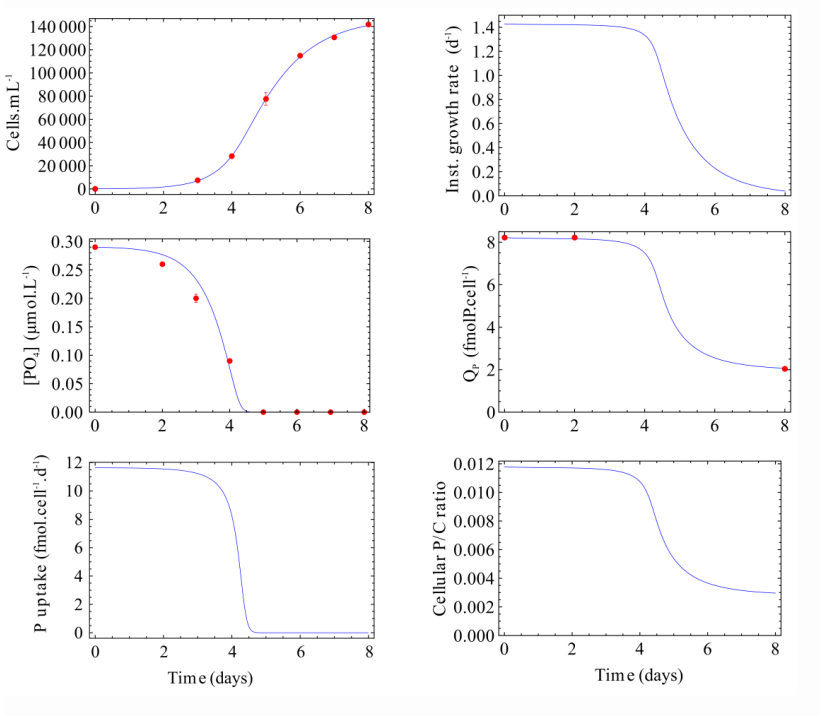

Figure 8. Model fitted to the data of the phosphate-limited cultures of Langer et al. (2013).

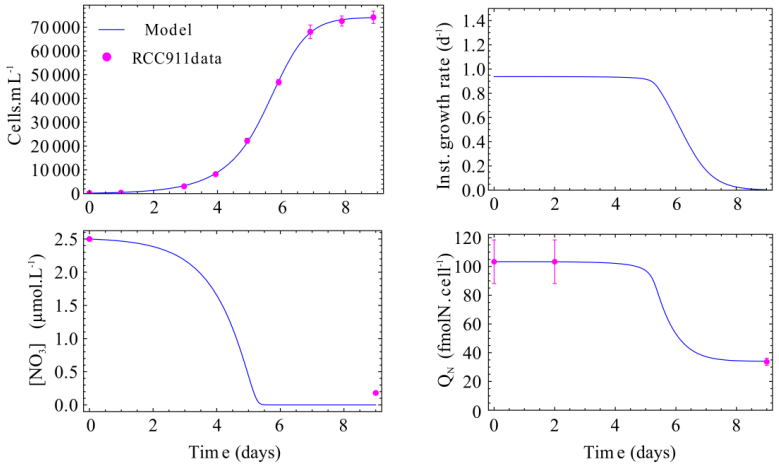

Figure 9. Model fitted to the data of the nitrate-limited cultures of strain RCC911 in high light conditions.

Biogeosciences Discuss., doi:10.5194/bg-2016-196, 2016
Manuscript under review for journal Biogeosciences
Published: 14 June 2016

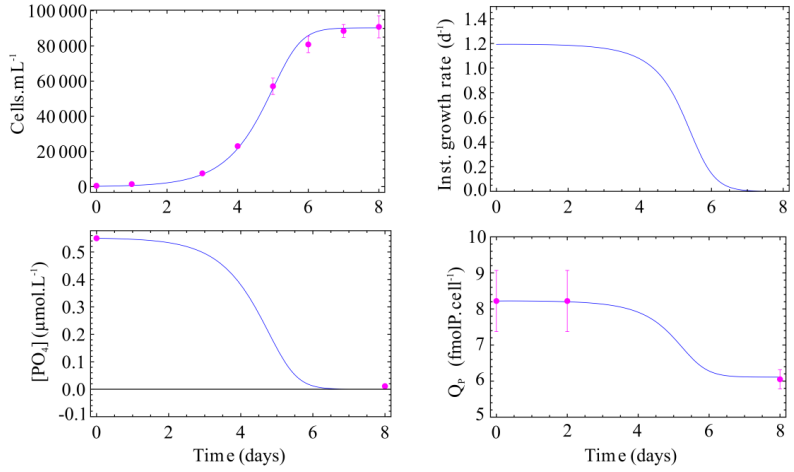

974

Figure 10. Model fitted to the data of the phosphate-limited cultures of strain RCC911 in high light conditions.

975

976

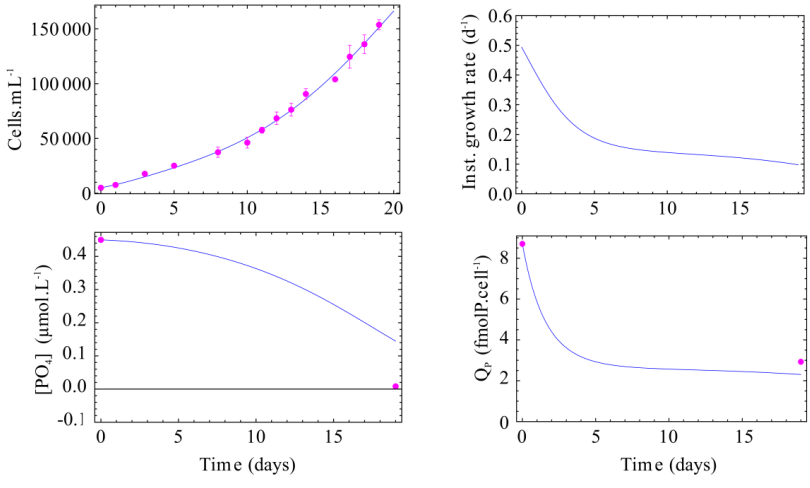

977

Figure 11. Model fitted to the data of the phosphate-limited cultures of strain RCC911 in low light conditions.

978

979

980

981

982

983

984

Biogeosciences Discuss., doi:10.5194/bg-2016-196, 2016
Manuscript under review for journal Biogeosciences
Published: 14 June 2016

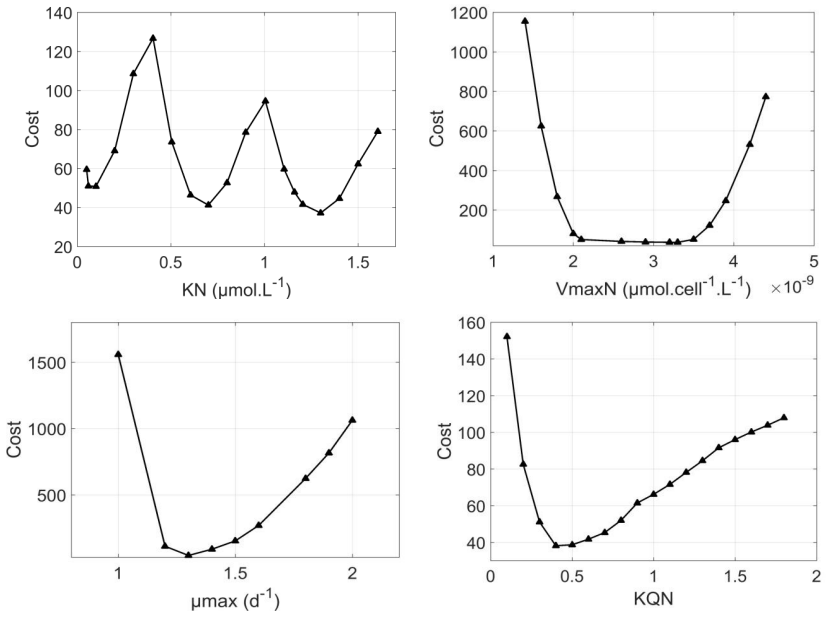

Figure 12. Variability of KN, VmaxN, µmax et KQN for the Langer et al. (2013) PML B92/11 experiment in nitrate-limited conditions.

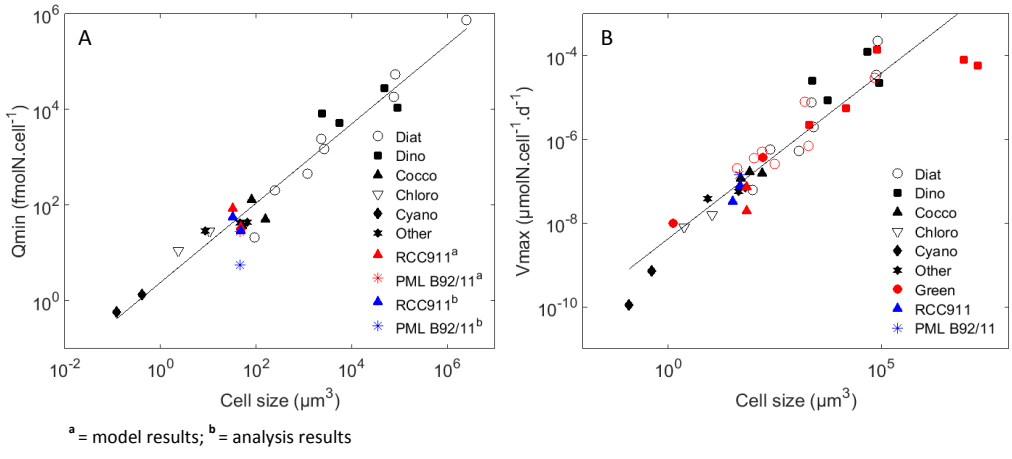

Figure 13. A) Minimum cellular quota Q_{min} for nitrate versus the cell volume. Data of Maranon et al. (2013) and the results of the present study (model simulation results in red and analytical results in blue. B) Maximum normalized surface uptake V_{maxN} for nitrate versus the cell volume. Data from Maranon et al. (2013) and Litchman et al. (2007) and the Droop model output for the experiments presented in this work.

Biogeosciences Discuss., doi:10.5194/bg-2016-196, 2016
Manuscript under review for journal Biogeosciences
Published: 14 June 2016

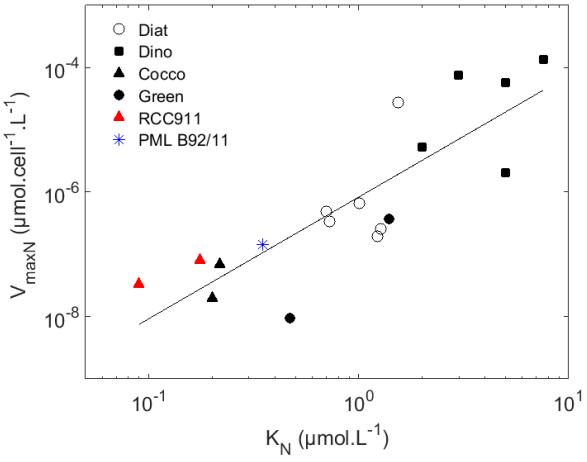

Figure 14. Data of Litchman et al. (2007) and results from the Droop model for RCC911 and PML B92/11 experiments in nitrate-limited conditions.

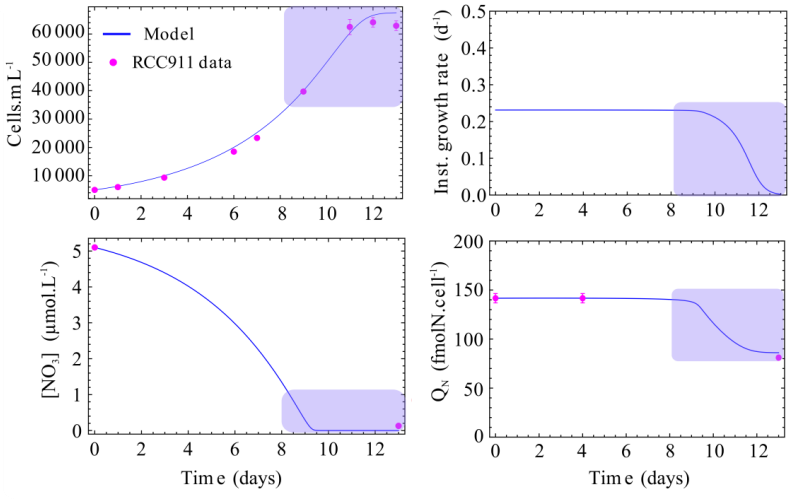

Figure 15. Model fitted to the data of the nitrate limited cultures on RCC911 strain in low light. The patch corresponds to the equivalent nitrate concentration in the BIOSOPE ecological niche of coccolithophores at the GYR station (between 150 and 200 m depth).

Biogeosciences Discuss., doi:10.5194/bg-2016-196, 2016
Manuscript under review for journal Biogeosciences
Published: 14 June 2016

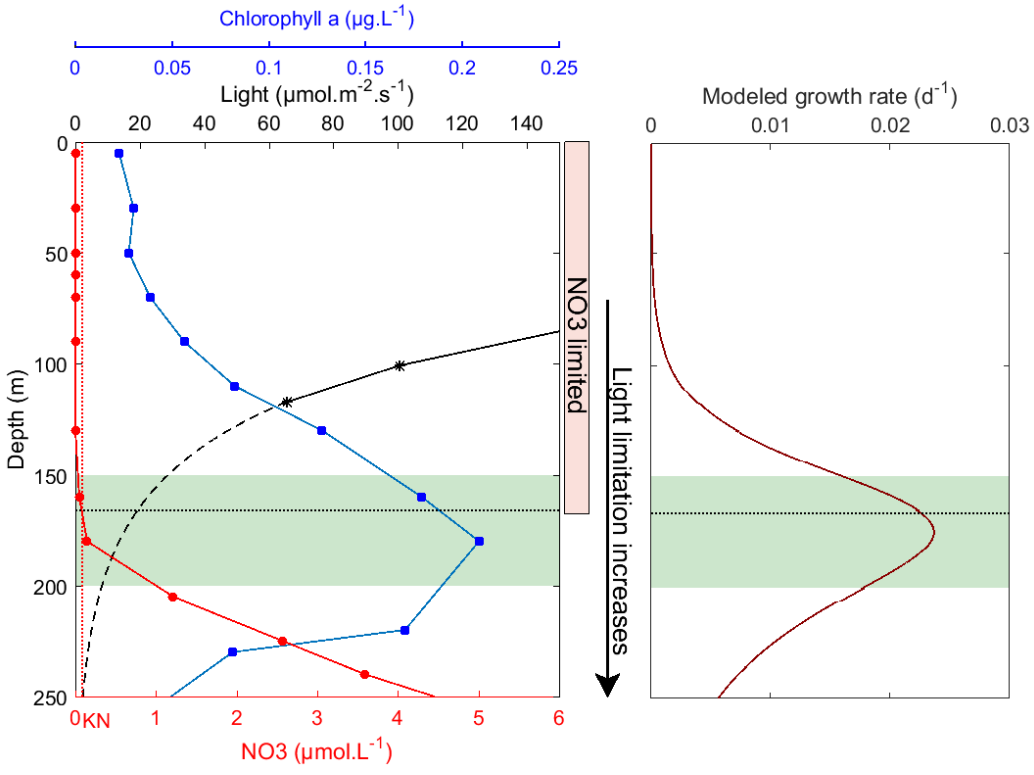

Figure 16. Left panel: In situ data (0 to 250 m) at the GYR station of the BIOSOPE transect (114.01° W, 26.06° S). Profiles of in situ measured chlorophyll a, PAR irradiance and nitrate concentration are shown. The dashed line represents an extrapolation of the irradiance between 117 m (last point measured) and 250 m considering a constant attenuation coefficient K_d (K_d=0.025 m^{-1} from Claustre et al., 2008) and a simple light calculation taken from MacIntyre et al. (2002). Dotted red line is the value of K_N calculated with the Droop model and dotted black line is the depth at which this K_N is observed. This depth also indicates the end of the nitrate limited part. Light limitation starts above the DCM and intensifies with depth. The green patch corresponds to the location of the maximum of coccosphere abundance taken from Beaufort et al. (2007) between 120° W and 107° W. The right panel shows the growth rate of *E. huxleyi* with depth at the GYR station (calculated using Eq. A8).

Biogeosciences Discuss., doi:10.5194/bg-2016-196, 2016
Manuscript under review for journal Biogeosciences
Published: 14 June 2016

1035 Table 1 : Growth rate, nutrient concentration, pH, DIC at the end of the experiments and shift in DIC
1036 compared with the initial DIC (averages from triplicate, n=3 for growth rates and nutrients analysis).

Sample	Growth rate[a]		NO3		PO4		pH		DIC		DIC shift
	d^{-1}	std	µmol.L^{-1}	std	µmol.L^{-1}	Std		std	µmol.kg^{-1}	std	%
High light											
Control	0,91	*0,03*	67,92	*1,98*	3,95	*0,12*	8,13	*0,01*	2177	*19,14*	2,1
PO4 lim	0,00		80,88	*0,35*	0,01	*0,00*	8,21	*0,01*	1894	*21,01*	12,1
NO3 lim	0,00		0,18	*0,03*	5,74	*0,00*	8,14	*0,00*	2060	*3,61*	4,7
Low light											
Control	0,28	*0,01*	79,10	*1,15*	4,90	*0,04*	8,13	*0,02*	2161	*7,55*	4,1
PO4 lim	0,13	*0,01*	75,25	*1,24*	0,01	*0,01*	8,30	*0,01*	1956	*8,33*	13,2
NO3 lim	0,00		0,13	*0,02*	5,83	*0,02*	8,09	*0,00*	2139	*4,16*	3,9

1037 [a] = cells are in exponential growth phase at the end of control experiments

1038

1039 Table 2 : Cellular carbon, nitrogen and phosphorus quotas (averages from triplicate; n=6 for cellular
1040 quotas measurements).

Sample	PIC		POC		PON		POP		PIC:POC		PON:POC		POP:POC	
	pg.$cell^{-1}$	std	pg.$cell^{-1}$	std	pg.$cell^{-1}$	std	pg.$cell^{-1}$	std		std		std		std
High light														
Control	3,46	*0,36*	10,80	*1,38*	1,45	*0,21*	0,16	*0,03*	0,32	*0,07*	0,11	*0,04*	0,0058	*0,0043*
PO4 lim	14,16	*3,19*	27,49	*1,53*	2,66	*0,10*	0,11	*0,01*	0,52	*0,14*	0,08	*0,01*	0,0015	*0,0005*
NO3 lim	7,06	*0,55*	15,77	*0,95*	0,40	*0,04*	0,07	*0,00*	0,45	*0,06*	0,02	*0,00*	0,0017	*0,0004*
Low light														
Control	0,89	*0,10*	10,98	*0,41*	1,98	*0,07*	0,18	*0,00*	0,08	*0,01*	0,15	*0,01*	0,0063	*0,0009*
PO4 lim	3,53	*0,25*	16,25	*0,56*	2,08	*0,08*	0,06	*0,00*	0,22	*0,02*	0,11	*0,01*	0,0014	*0,0003*
NO3 lim	3,15	*0,13*	9,67	*0,21*	0,79	*0,02*	0,11	*0,00*	0,33	*0,02*	0,07	*0,00*	0,0044	*0,0006*

1041

1042 Table 3 : Cell, coccosphere volume and DSL (n=300 for coccosphere/cell measurements and n=100 for
1043 coccoliths measurements) at the end of our experiments. No measurement of coccosphere and DSL
1044 for control experiment in low light.

Sample	Cell volume		Coccosphere volume		DSL	
	µm^3	std	µm^3	std	µm	std
High light						
Control	49,97	16,38	109,5	23,3	3,05	*0,24*
PO4 lim	77,21	19,89	260,5	88,2	3,27	*0,27*
NO3 lim	47,33	11,13	139,2	41,2	2,78	*0,24*
Low light						
Control	33,69	10,09				
PO4 lim	55,64	14,42	168,6	50,0	3,10	*0,27*
NO3 lim	31,09	8,25	85,4	24,7	2,64	0,21

1045

Biogeosciences Discuss., doi:10.5194/bg-2016-196, 2016
Manuscript under review for journal Biogeosciences
Published: 14 June 2016

1046 Table 4: Value of $Q_{N/P}^{min}$ (which corresponds to the cellular PON (POP) at the end of the experiment:
1047 values measured and calculated) and the parameters obtained with the best-fit indicated for N and P
1048 limited experiment (high light: HL and low light: LL).

			$Q_{N/P}^{min}$		Best-fit			
Strain	**Light**	**Limitation**	**Analysis** *fmol.cell^{-1}*	**Calculation** *fmol.cell^{-1}*	**$V_{maxN/P}$** *µmol.cell^{-1}.d^{-1}*	**$K_{N/P}$** *µmol.L^{-1}*	**μ_{max}** *d^{-1}*	**$KQ_{N/P}$**
PML B92/11		**NO_3**	5,71	27,7	$1,46.10^{-7}$	0,35	1,3	0,39
PML B92/11		**PO_4**	1,935	2,04	$1,37.10^{-8}$	0,051	1,57	0,98
RCC911	**HL**	**NO_3**	28,57	31,28	$8,02.10^{-8}$	0,175	1	0,215
RCC911	**HL**	**PO_4**	3,464	5,931	$1,86.10^{-8}$	0,49	1,6	1
RCC911	**LL**	**NO_3**	56,14	78,99	$3,34.10^{-8}$	0,09	0,2	0,3
RCC911	**LL**	**PO_4**	1,968	2,875	$7,43.10^{-10}$	0,45	0,5	0,45

1049
1050

1051 Table 5 : In situ environmental conditions at the Deep ecological niche at 200 m depth at the GYR
1052 station and initial conditions of the nutrient and light-limited experiment presented in this study.

	BIOSOPE	**RCC911 exp**
T (°C)	17,5-20	20
Light (µmol.m^{-2}.s^{-1})	< 20	30 (*Low light*)
pCO_2 (µatm)	~ 400	~ 400
NO_3 (µM)	~ 1	~ 3
PO_4 (µM)	~ 0,2	~ 0,4

1053